Rylene Dyes

DOI: 10.1002/anie.200902532

The Rylene Colorant Family—Tailored Nanoemitters for Photonics Research and Applications

Tanja Weil, Tom Vosch, Johan Hofkens,* Kalina Peneva, and Klaus Müllen**

Keywords:
biolabeling · nanoemitters · perylene dyes · photonics · single-molecule spectroscopy

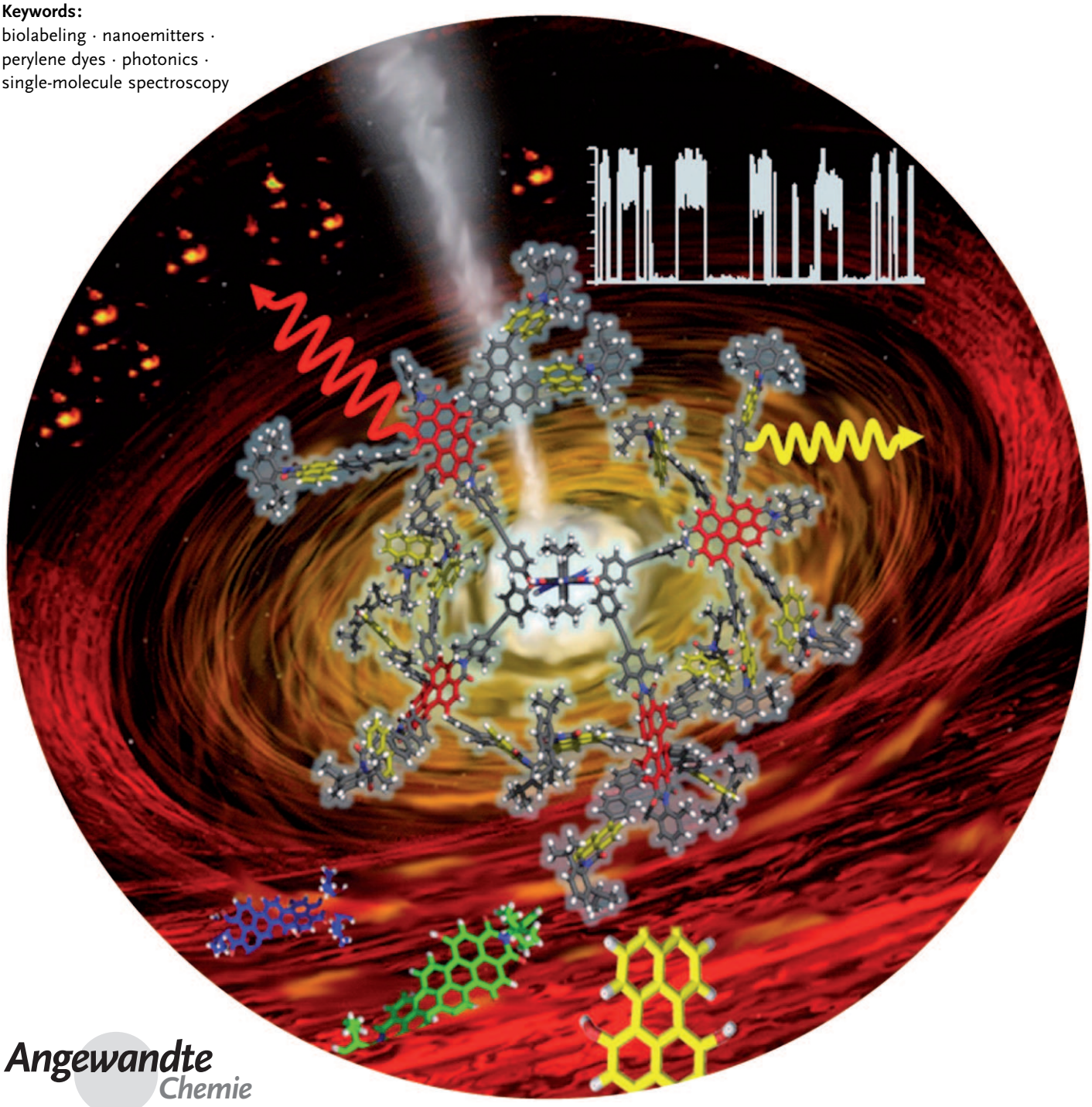

This Review summarizes the latest advances in the field of rylene dyes and rylene nanoemitters for applications in photonics, and describes the influence of the dye design on the optical properties, the self-assembly, the molecular interactions, as well as the labeling specificity of the compounds. The interplay between tailored (macro)molecular design and bulk/single-molecule spectroscopy enables complex processes to be explained, for example, the kinetics of energy-transfer processes or (bio)catalysis. Such investigations are essential for the ultimate design of optimized nanoemitters, and require a close cooperation between spectroscopists and preparative organic chemists.

From the Contents

1. Introduction

Dye chemistry is considered one of the oldest and most explored areas in industrial organic chemistry. Traditional applications consist of staining or coloration of textiles and consumer goods.[1–4] A large variety of dyes are commercially available and one could question whether there is still a need for the preparation of new chromophore systems. In recent years, an emerging area of growth in colorant chemistry has involved dyes for use in "high-level photonic applications", for example, dyes for liquid-crystal displays, lasers, solar-energy converters, or bioimaging. Such dyes are termed "functional dyes" and their design is not merely directed towards color tuning. The fine regulation of band-gap energies, self-organization, charge-carrier mobilities, photostability, or the attachment of molecular recognition units are considered adjustable parameters when designing novel chromophores.[5–7] Most common chromophores, such as fluoresceins, rhodamines, several 4,4′-difluoro-4-bora-3a,4a-diaza-*s*-indacenes (bodipy dyes), and most cyanines, are dyes that are characterized by relatively narrow absorption and emission bands, high molar absorption coefficients, and moderate to high fluorescence quantum yields, thus making them attractive for a wide range of applications.[8] However, with very few exceptions, such as acridone dyes, the fluorescence lifetimes and photostabilities of organic dyes are limited, thus precluding efficient temporal discrimination of short-lived fluorescence interference from scattered excitation light.[8] In this context, rylene dyes have attracted a great deal of attention since they are not only superb colorants, but they also possess exceptional chemical, thermal, photochemical, and photophysical stability in combination with high extinction coefficients.[9–13] They are based on naphthalene units linked in the *peri* position. Rylene dyes can be described as poly(*peri*-naphthalene)s if their chromophore system is envisioned as a polymer. Their nomenclature was introduced by Clar, and is depicted in Figure 1.[14] Functionalized rylene derivatives were explored for demanding applications such as optoelectronic[15–18] and photovoltaic[19–25] devices, thermographic processes,[26,27] energy-transfer cascades,[28] light-emitting diodes,[29–32] and near-infrared-absorbing systems.[33] They have been particularly successful for single-molecule investigations.

This Review summarizes recent advances in the design of rylene chromophores and rylene nanoemitters. Furthermore, we highlight the impact of the chromophore design on the resulting performance by focusing on their optical properties, self-organization, and molecular interactions, as well as the specificity of the resulting functional dyes. In this context, the term nanoemitter refers to a fluorescent macromolecule with a length scale mainly between 1 and 50 nm, which is in contrast to typical chromophores which have dimensions below 1 nm. In particular, the synergy between tailored molecular and macromolecular design on the one hand, and bulk spectroscopy or single molecule spectroscopy investigations on the other hand, provides absorption, emission, or excitation spectra of (single) nanoobjects that facilitate the

[*] K. Peneva, Prof. Dr. K. Müllen
Max Planck Institute for Polymer Research
Ackermannweg 10, 55128 Mainz (Germany)
Fax: (+49) 6131-379-350
E-mail: muellen@mpip-mainz.mpg.de
Prof. Dr. T. Weil
National University of Singapore
3 Science Drive 3, 117543 Singapore (Singapore)
Fax: (+65) 6779-1691
E-mail: chmweilt@nus.edu.sg
Prof. Dr. J. Hofkens
Katholieke Universiteit Leuven
Celestijnenlaan 200f, 3001 Heverlee (Belgium)
Fax: (+32) 16-327990
E-mail: Johan.Hofkens@chem.kuleuven.be
Prof. Dr. T. Vosch
University of Copenhagen
Universitetsparken 5, 2100 Copenhagen (Denmark)

determination of their positions or the three-dimensional orientations of their transition dipole moments.[18,34] By experimentally monitoring individuals rather than populations, the origin of complex behavior, for example, kinetics in energy-transfer processes or (bio-)catalysis can be elucidated and opens up a deeper insight to the origin and nature of non-uniformities. Such investigations are essential for the ultimate design of optimized nanoemitters, and require a close cooperation between spectroscopists and preparative organic chemists.

2. Spectral Fine-Tuning of Functional Rylene Dyes

The transition from insoluble rylene pigments to soluble rylene dyes is achieved by specific functionalization of the rylene scaffold. The major difference between dyes and pigments is their solubility, that is, the tendency to dissolve in a liquid. Dyes are usually soluble in organic or aqueous solvents, whereas pigments are generally not soluble in water, oil, or other common solvents. Extending the aromatic scaffold of the chromophore core results in a stepwise bathochromic shift of the absorption and emission maxima, which usually comes with a significant reduction in the solubility and processability of higher order rylenes.[18,35] However, the large π-conjugated systems of rylene dyes provide a versatile synthetic basis for further functionalization. Different kinds of substituents can be introduced at the *peri* as well as the *bay* positions of the perylene core (Figure 1).[35] The nature of the substituents as well as the position at which they are attached to the rylene core has a strong impact on the resulting solubility as well as the optical properties, such as HOMO/LUMO energies, absorption wavelengths (λ_{max}), and the spatial properties of the molecular orbitals.[18,35] In this way, the introduction of substituents offers access to a large portfolio of tailored functional rylene chromophores, which can be functionalized for the desired application, for example, single-molecule investigations of energy and electron-transfer processes, devices, biolabeling, staining, or FRET biosensors.[18,35] In this Review, the most important concepts for achieving functional rylene dyes will be introduced and the impact of different functionalization strategies on selected molecular properties such as their optical characteristics, photostabilities, intramolecular charge transfers, or interaction with surfaces will be highlighted.

Tanja Weil studied chemistry (1993–1998) at the TU Braunschweig (Germany) and the University of Bordeaux I (France) and completed her PhD at the MPI for Polymer Research under the supervision of K. Müllen. In 2003 she received the Otto Hahn Medal of the Max Planck Society. From 2002 to 2008 she advanced from Section Head of medicinal chemistry to Director of Chemical Research and Development at Merz Pharmaceuticals GmbH (Frankfurt). In 2005 she was also appointed to the MPI for Polymer Research and in 2008 she became an Associate Professor at the National University of Singapore. Since 2010 she has been Director of the Institute of Organic Chemistry III and Macromolecular Chemistry at Ulm University.

Tom Vosch completed his PhD in chemistry at the Catholic University of Leuven in 2003. After postdoctoral research with R. Dickson at the Georgia Institute of Technology (2005–2006), he returned to Leuven to the group of J. Hofkens, where he focused on single molecule studies. In 2010 he was appointed Associate Professor at the Nano-Science Center/Department of Chemistry at the University of Copenhagen. His research interests include single-molecule and ensemble spectroscopy, fluorescence and Raman spectroscopy, and silver cluster fluorescence.

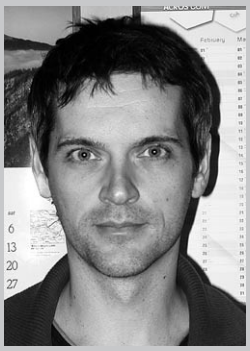

Johan Hofkens studied chemistry and completed his PhD at the Catholic University of Leuven. After postdoctoral research with H. Masuhara at Osaka University and P. F. Barbara at the University of Minneapolis, he returned to Leuven, where he supervised the Single Molecule Unit in the group of F. de Schryver. In 2005 he was appointed Research professor in Leuven and recently promoted to Full Professor. His research interests include fast spectroscopy, (single-molecule) fluorescence spectroscopy and nanoscopy, as well as the application of these techniques to materials science and biosciences.

Kalina Peneva studied chemistry at the University of Sofia. She joined the group of K. Müllen at the MPI for Polymer Research in 2004 and completed her PhD in 2008. After one year postdoctoral research as a Research Scientist at Ciba, she became a project leader at the MPI for Polymer Research. Her research interests include the design of biobybrid systems and their applications.

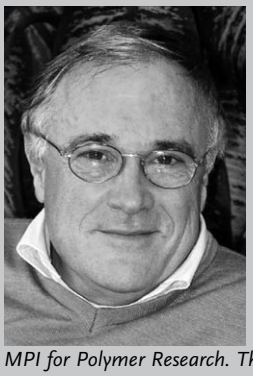

Klaus Müllen obtained a diploma in chemistry in 1969 at the University of Cologne and completed his PhD in 1972 on EPR spectroscopy at the University of Basel under the supervision of F. Gerson. After postdoctoral research at the ETH Zurich with J. F. M. Oth on dynamic NMR spectroscopy and electrochemistry, he completed his Habilitation there in 1977. In 1979 he became Professor in the Department of Organic Chemistry in Cologne, and in 1983 took the Chair in Organic Chemistry at the University of Mainz. In 1989 he became director of the MPI for Polymer Research. The focus of his research is synthetic macromolecular chemistry and materials science. 2008–2009 he was President of the GDCH.

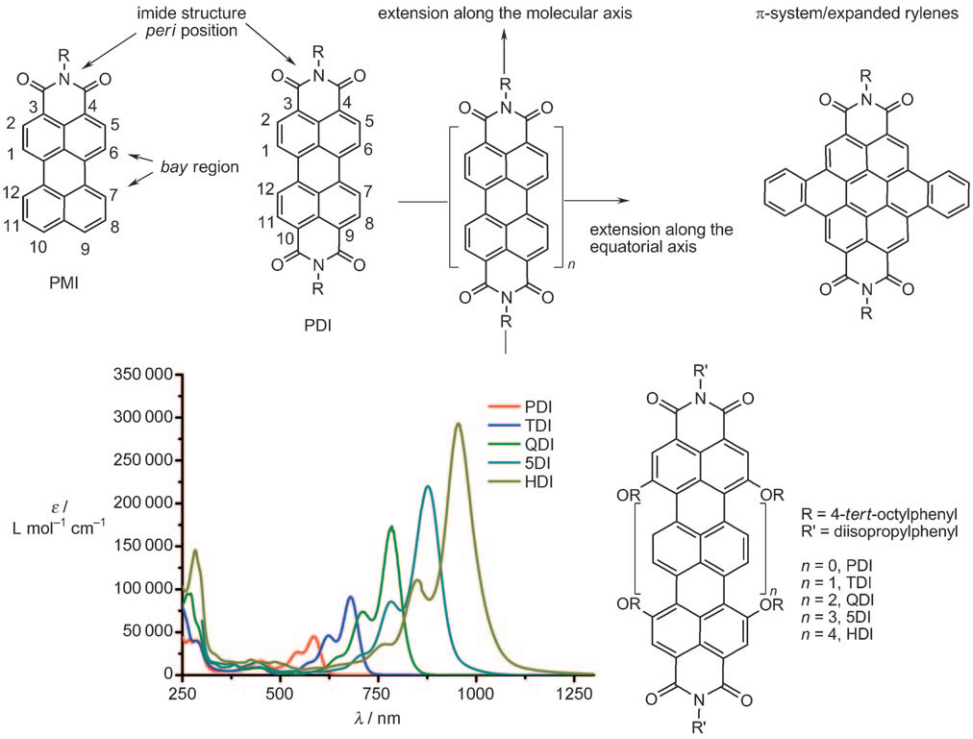

Figure 1. Top: Chemical structures of unsubstituted peryleneimide chromophores: Perylene-3,4-dicarboximide (PMI) and perylenebis(dicarboximide) (PDI), illustration of the *bay* and *peri* positions, as well as the concept of achieving higher order rylenes by extending the aromatic scaffold. Bottom: Absorption spectra of the entire tetraphenoxy-substituted rylenediimide series in $CHCl_3$: perylenebis(dicarboximide) (PDI), terrylenebis(dicarboximide) (TDI), quaterrylenebis(dicarboximide) (QDI), pentarylenebis(dicarboximide) (5DI), hexarylenebis(dicarboximide) (HDI).

2.1. Higher Order Rylene Dyes

Synthetic approaches to obtain a homologous series of rylene dyes from perylenebis(dicarboximide) to hexarylenebis(dicarboximide)[33] (Figure 1) have been developed. The extension of the aromatic system along the long molecular axis from perylene- (PDI, $n=0$), to terrylene- (TDI, $n=1$)[36] and quaterrylenebis(dicarboximide)s (QDI, $n=2$)[37,38] generally induces a bathochromic shift of about 100 nm per additional naphthalene unit (reaching an absorbance maximum of 780 nm for the quaterrylene). In addition, a nearly linear increase in the extinction coefficient up to $170\,000\,M^{-1}cm^{-1}$ for rylene homologues has been achieved. Very recently, the synthesis of two higher rylene homologues, pentarylene- ($n=3$, $\lambda_{max}=877$ nm) and hexarylenebis(dicarboximide)s ($n=4$, $\lambda_{max}=950$ nm), each showing an intensive absorption in the near infrared (NIR) region, were reported.[33,39] All rylene chromophores display relatively narrow absorption and emission envelopes.

The access to different rylene homologues allows their application as donor as well as acceptor chromophores for both Förster-type energy-transfer (FRET) and electron-transfer (ET) studies and offers the opportunity to selectively excite a particular rylene homologue (for example, PDI, TDI, QDI). This feature is particularly attractive for multifluorophore labeling experiments and energy-transfer investigations.

Benzannulation of the *bay* region of rylenebis(dicarboximide)s enabled new chromophores with expanded π systems along the equatorial axis to be synthesized (Figure 1 a).[35,40,41] These are characterized by significant hypsochromic absorption shifts, compared to their parent rylenebis(dicarboximide)s, while the excellent photostabilities and high fluorescence quantum yields are retained.[35,40,41]

2.2. Phenoxylation of Rylene Dyes

The introduction of substituents such as phenoxy groups at the *bay* position has been widely applied and it allows control over the band gaps and improves their solubility and processability.[42] Substitution with phenoxy arms in the *bay* position is one of the most frequently used synthetic methods for the entire family of rylene dyes (PMI, PDI, TDI).[42] It is a convenient way to increase the solubility of these colorants and prevent aggregation through π stacking.[43] For example, substitution in the *bay* area with large phenoxy-based dendritic arms not only improves the solubility in organic solvents but has also been found to protect the core chromophore from oxygen or radicals.[48] This strategy has been employed not only in single-molecule studies[44] but also in the generation of femtosecond laser-induced shockwave production of nanoparticles.[45,46] At the same time, the photophysical and redox properties of the chromophores are changed. Compared to the unsubstituted rylene dyes, for example, **1**, the *bay*-substituted perylene derivatives **2** and **3** (Figure 2) reveal less vibronic fine structure, bathochromically shifted absorption and emission spectra, different fluorescence lifetimes, and a pronounced increase in the $S_0 \rightarrow S_2$ absorption strength. This behavior is due to the electron-donating character of the phenoxy substituents and this effect can be enhanced further by increasing the donating character of the substituents by the introduction of *meta* or *para*-methoxy groups (**2b**,**c**; Figure 2).[47] In the case of both PDI and TDI chromophores, the attachment of more-bulky substituents results in a slight twisting of the planar core of PDI chromophore **3** (Figure 2)[48–50] as well as multiexponential fluorescence decays because of the conformational freedom of the substituents[49,51] (Table 1). Furthermore, the properties of higher excited states are influenced by the phenoxy groups. In

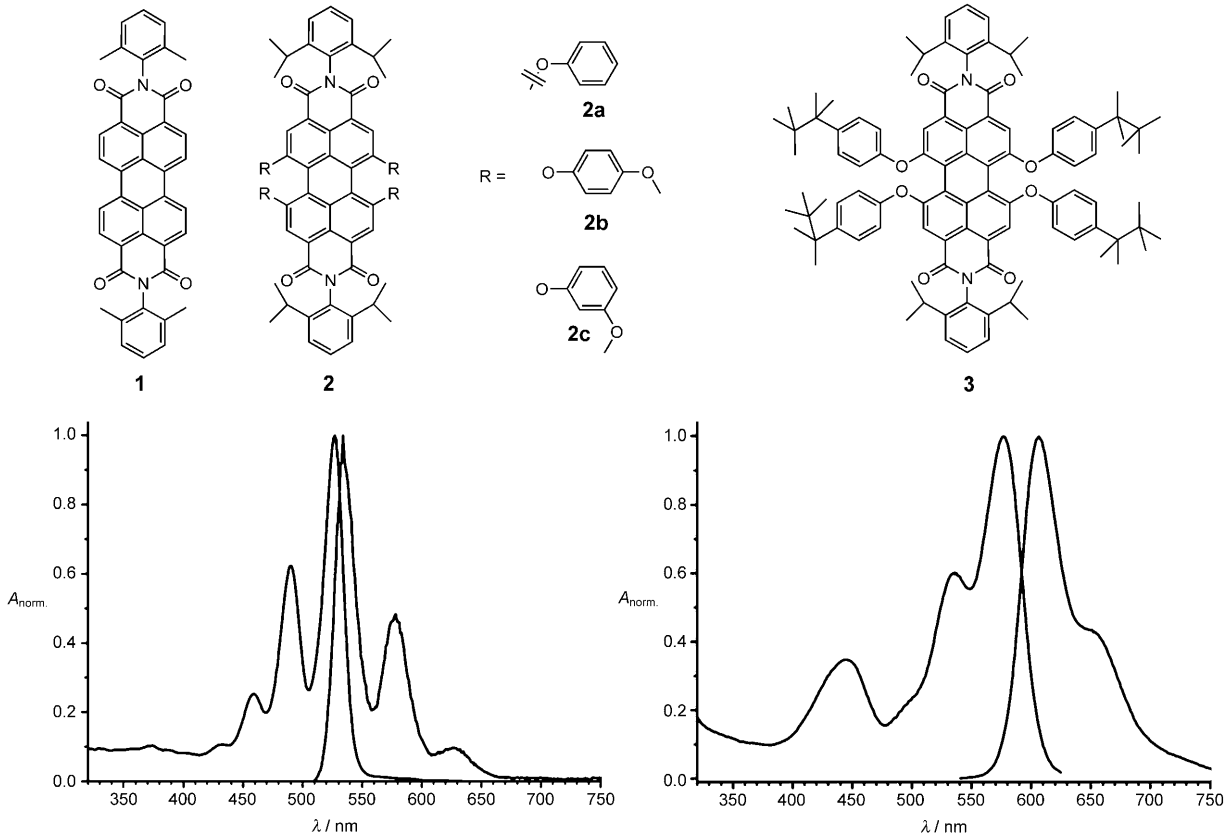

Figure 2. Molecular structures and stationary spectra of an unsubstituted (**1**, left) and a *bay*-substituted (**3**, right) PDI chromophore. The difference in the vibronic fine structure is clear: The pronounced band at 440 nm in the absorption spectrum on the right is the $S_0 \rightarrow S_2$ absorption band.

Table 1: Maxima of the ground-state absorption and emission spectra, extinction coefficients, and the fluorescence decay times of three dyes in toluene which are partially substituted in the *bay* region with phenoxy groups.

		S_0–S_1 Absorption maximum [nm]	S_0–S_2 Absorption maximum [nm]	Emission maximum [nm]	ε [L mol^{-1} cm^{-1}]	Fluorescence decay time [ns] and amplitudes [%]
peryleneimide	unsubstituted (**4**)	520	–	560	38300	4.2
	substituted (**5**)	530	–	575	41000	4.0
perylenediimide	unsubstituted (**1**)	525	–	536	–	3.7
	substituted (**3**)	580	440	606	42000	5.5 (94%) 0.55 (6%)
terrylenediimide	unsubstituted (**12**)[a]	651	–	670	85000	3.2
	substituted (**38**)[b]	677	450	710	85000	3.2 (80%) 0.9 (10%) 0.115 (10%)

[a] Structure with 2,6-diisopropylphenyl group instead of the alkyl chain. [b] Structure without sulfonyl groups.

the case of the phenoxy-substituted PMI **5**, the $S_1 \rightarrow S_n$ absorption spectrum is substantially shifted, which leads to less overlap with the fluorescence spectrum (Figure 3), and hence a reduced singlet–singlet annihilation rate is observed.

The already excellent photostability of rylene dyes is further improved by the phenoxy groups, for reasons which are not fully understood. This property is particularly useful for measurements on single molecules (see Section 3).[52]

2.3. Rainbow Perylene Monoimides by "Push-Pull" Substitution

The introduction of substituents in the 1-, 6-, and 9-positions of the *N*-(2,6-diisopropylphenyl)perylene-3,4-dicarboximide core resulted in the generation of novel perylene dyes **6**–**10** (Figure 4).[53] A "push-pull" family of perylenes (**6**, **7**) was achieved through a three-step reaction[53] by using the carboxydiimide group of PMIs as an electron acceptor and selectively functionalizing the 1-, 6-, and 9-positions with

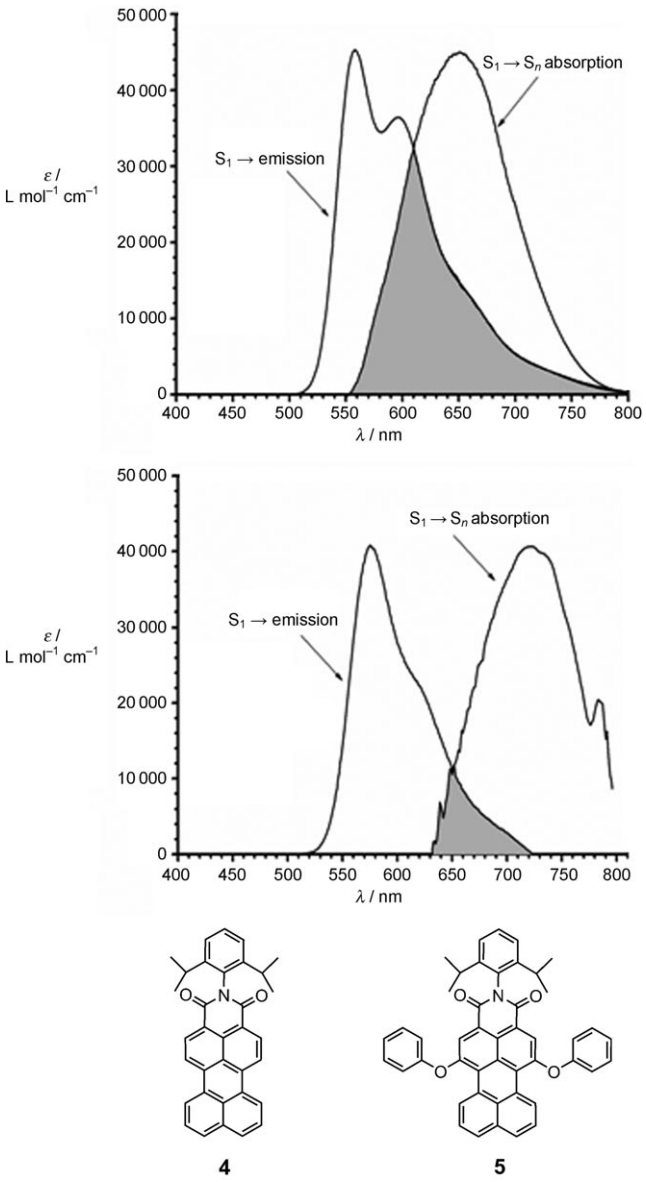

Figure 3. Emission and $S_1 \rightarrow S_n$ absorption spectrum of top: PMI dye **4** and bottom: phenoxy-substituted PMI **5**. The gray area indicates the overlap between the two spectra, which is one of the determining factors for the efficiency of singlet–singlet annihilation amongst identical chromophores.

different electronic donors (Figure 4). These dyes exhibit a rainbow of colors as well as tunable spectroscopic and electrochemical properties. Their absorption maxima can be successfully shifted throughout the entire visible region by changing the donor and acceptor strengths and the position at which the substituents are attached to the scaffold of the perylenes. Moreover, orbital calculations and optical measurements indicate that an intramolecular charge transfer occurs when the perylene core is functionalized with a donor and an acceptor substituent at opposite *peri* positions.[53] Such dyes, thus, become relevant candidates as sensitizers in dye-sensitized solar cells (DSSCs). On the basis of these results the highly efficient perylene sensitizer **11** was designed by carefully selecting the appropriate substituents in the *bay* and *peri* positions. These PMIs can be modified with anhydride groups for use in DSSCs. Saponification then leads to dicarboxylic acid groups, which can attach to TiO_2 surfaces. The perylenemonoanhydride (PMA) **11** reveals an incident monochromatic photon-to-current conversion efficiency of 87% as well as a power conversion efficiency of 7.2% when included in DSSCs.[53] The fine-tuning of the substituents provides a powerful way to generate new perylene sensitizers with stronger intramolecular charge transfer (ICT), more suitable HOMO or LUMO energies, and more favorable light absorption properties for solar conversion.

In this section, we have discussed the most prominent ways to tailor the optical properties of rylene dyes through the introduction of functional groups at distinct positions of the chromophore core. In the following section the influence of the environment on the optical properties of single rylene dyes will be elaborated. The sensitivity of rylene chromophores towards their nanoenvironment combined with their high photostability means that these dyes can serve as efficient individual reporters of their local surroundings. Indeed, multiparametric single-molecule spectroscopy has proven to be an excellent tool to probe the local environments of individual dyes.[34,51]

3. Rylene Emitters as Single-Molecule Reporters of their Local Nanoenvironments

3.1. Single-Molecule Investigation of Rylene Emitters

One of the greatest challenges is still the visualization of a single molecule. Performing experiments at the single-molecule level enables information to be obtained that would otherwise not be observed from the ensemble average.[54–60] In this way, single-molecule measurements provide direct access to subpopulations in an ensemble, enable the detection of rare events, and lift the requirement of synchronization in the study of time-dependent phenomena. Ideally, a molecule used in single-molecule spectroscopy (SMS) has a high molar absorption coefficient, quantum yields close to unity, and good photostability.[61] When these parameters are satisfied, almost every absorbed photon will result in an emitted photon and the molecule can go through a high number of absorption/emission cycles before an irreversible photoproduct is formed (photobleaching).[62–65] As a general rule, the lower limit of the product of the extinction coefficient (ε) and the fluorescence quantum yield ($\Phi_{fl}\varepsilon \times \Phi_{fl}$ at the applied excitation wavelength is set at $20000\,M^{-1}cm^{-1}$ for a good single-molecule assay.[61] As mentioned before, rylene dyes easily pass this threshold. Since they outperform other dye molecules at the single-molecule level in terms of "survival time", they are the preferred molecules for many experimentalists.[58,66–69]

Amongst the rylene family, phenoxy-substituted PDI **3** (Figure 2) is probably one of the most robust molecules, with survival times from minutes to tens of minutes under normal single-molecule excitation conditions ($1\,kW\,cm^{-2}$).[48,52] A characteristic time trace (detected number of counts per predefined time interval as a function of time) of a single PDI

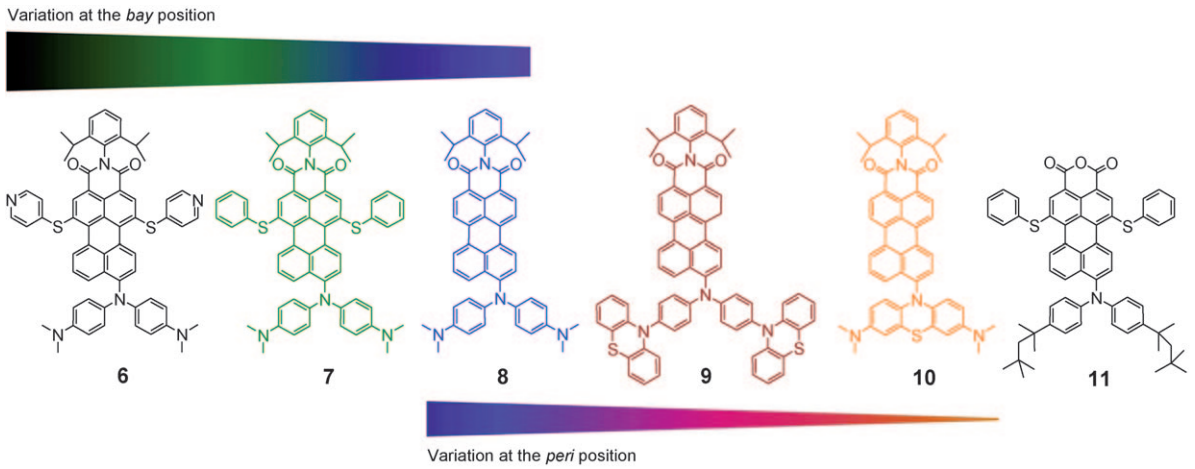

Figure 4. Chemical structures of "push-pull" PMIs **6**–**10** and perylene sensitizer **11**.

molecule embedded in a polymethylmethacrylate (PMMA) polymer film is shown in Figure 5. A typical observation in the study of immobilized single molecules is that the fluorescence rate is not constant over time, that is, the fluorescence intensity changes as a function of time. This phenomenon is referred to as blinking and has been observed to occur on time scales ranging from microseconds to tens of seconds.[70–72] PDI, like any organic molecule, blinks on a timescale of

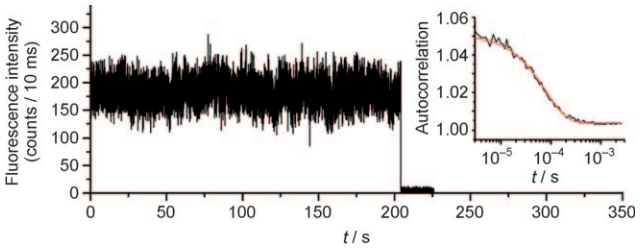

Figure 5. Time trajectory of a single PDI molecule in a PMMA thin film. The inset shows an intensity correlation function of the trajectory and gives a blinking process with a time constant of 77 μs, which is attributed to formation of a triplet.

tens to hundreds of microseconds (see Figure 5, inset). The physical process responsible is thought to be intersystem crossing (ISC), and the microsecond timescale is the typical time that organic molecules reside in the triplet state when immobilized in a polymer film.[73–75] Unlike many other molecules, PDI rarely shows long off times (none are observed in the time trace shown in Figure 5). The general consensus regarding the cause of this effect is that such off times are due to intermolecular charge transfer between the single molecule and the surrounding environment.[70,72]

The observed photostability and lack of complex inherent dynamics allows rylene dyes to be used as reporter molecules of their local nanoenvironment in a wide variety of material-science-related single-molecule studies. Although the blinking of single molecules has been regarded as a possible limitation for the applicability of SMS, it has recently been shown that this previously unwanted property can become an advantage: The blinking of single molecules can be employed for super-resolution microscopy or nanoscopy. For further information on this topic we refer to the corresponding literature.[76–88]

3.2. Following Polymer Dynamics Near the Glass-Transition Temperature T_g with Rylene Dyes

The glass transition and the associated glass-transition temperature T_g are widely known and well-studied concepts in polymer physics. Physical properties, such as viscosity, change abruptly, often over orders of magnitude, at the glass-transition temperature.[61,89] This unique property of glass formers originates from complicated relaxation processes of polymer chains. For a number of years, researchers have attempted to monitor relaxation processes in glass formers by embedding a single dye molecule in a polymer of interest.[90–95] The idea is that small rotational motions of the embedded dye would be able to report back on the relaxation process of the polymer under investigation. Several microscopy techniques have been developed over the last years to monitor the rotational motion of single molecules in three dimensions. One such method is the defocused wide-field imaging technique, which provides direct pictures (referred to as patterns) of a given 3D orientation of a molecule (Figure 6). The principles and merits of this technique have been reviewed recently.[61,96]

By using defocused imaging and **3** as a reporter molecule, the rotational motion of a single emitter **3** could be followed. The analyzed sequence of rotational motions allows a correlation function to be constructed, and subsequent curve fitting can then extract the relevant relaxation times of the polymer.

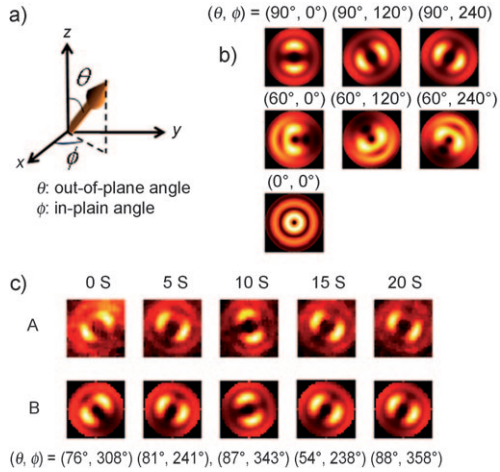

Figure 6. a) Description of the reference frame and angles in the defocused imaging experiments. b) Calculated defocused patterns (defocusing depth of 1 micrometer) for different orientations of the transition dipole moment associated with a PDI molecule. c) Defocused images of **3** in a PnBMA thin film at 310 K. Experimental emission patterns (top row) and corresponding simulated patterns (bottom row). The polymer used is PnBMA:poly(*n*-butyl methacrylate) with $M_w = 10200\ g\,mol^{-1}$ and $M_w/M_n = 1.06$.

3.3. Visualization of Mesoporous Films by Using an Asymmetric TDI Dye

Related nanoreporters based on a TDI scaffold have been designed which allow complex and industrially important materials, such as mesoporous silicates in which channels are present, to be studied. The extended size of the TDI scaffold, which induces a red-shift of the emission and absorption spectra compared to PDI, makes it an attractive emitter for single-molecule investigations because of the reduced scatter and fewer problems with impurities. A desymmetrized TDI nanoreporter was designed by introducing a bulky diisopropylimide group and an *N*-alkyl chain at the *peri* position of the TDI dye (Figure 7a). This TDI emitter is highly lipophilic and diffuses freely in organic solvents such as chloroform. In addition, the presence of the four oxygen atoms of the imide structure allows the formation of secondary interactions with their surroundings.

The diffusion of TDI **12** within a porous network templated by cetyl trimethylammonium bromide (CTAB) was recorded by the simultaneous observation of the orientational and spectral dynamics of the TDI molecules. This provided direct information about the influence of the local environment on the guest molecule (Figure 7b,c).[12,97,98] In the presence of air, the TDI reporter molecules are nearly immobile, which might be due to an interaction with the oxygen atoms of the carbonyl groups, whose lone pair of electrons can interact with the positively charged heads of the CTAB molecules or active silanol groups (Figure 7d). If the solvent is changed to chloroform, which is a favorable solvent for the lipophilic TDI dye, small solvent molecules likely form a lubricant-like phase inside the pores (Figure 7e). As a result, the TDI molecules are solvated and diffuse along the pores.

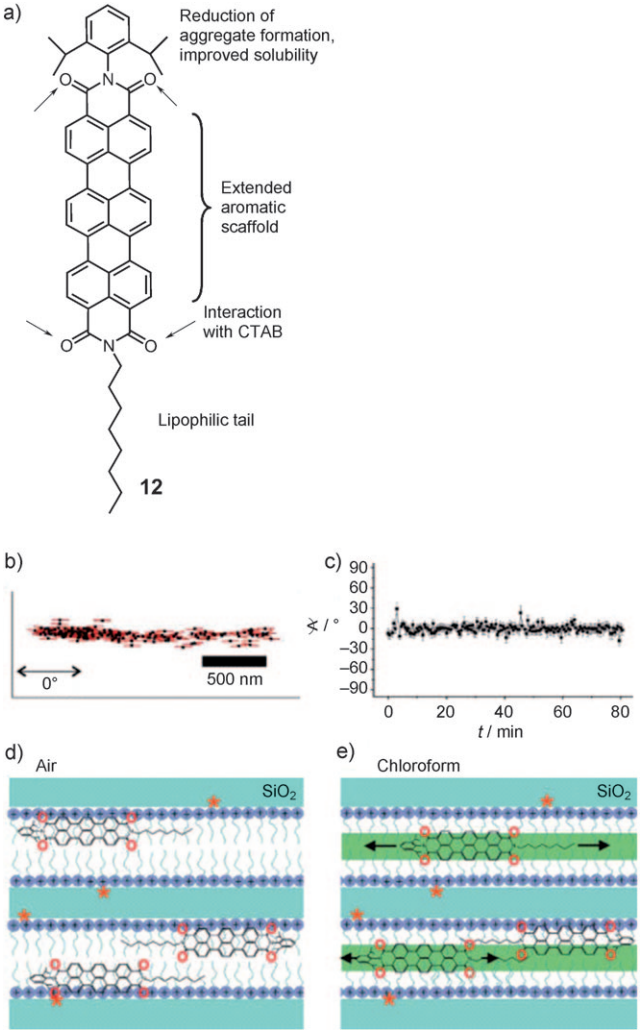

Figure 7. a) Chromophore design of the asymmetric TDI derivative **12**. b) Trajectory of **12** and the structure-directing agent CTAB. c) Calculated angular time trajectory of **12**. d) Schematic representation of TDI molecules immobilized in the mesoporous material in air; *: active silanol groups. e) TDI molecules in the mesoporous material in the presence of chloroform; the TDI molecules are solvated (green stripe) and diffuse along the channels, and their "walk" is occasionally interrupted by adsorption events.

The orientation of the single TDI molecules (long axis parallel with the channels) and their trajectories map directly the direction of the channels and the domains of parallel channels. The high photostability of the TDI reporters in mesoporous materials allows individual molecules to be tracked for over 1000 s. In this time interval, molecules can diffuse over considerable distances. These data hold great importance for the optimization of the synthesis of highly structured molecular membranes or molecular sieves. It was also shown that information on the channels obtained with single-molecule microscopy could be overlaid with structural information obtained by electron microscopy techniques, thereby validating fluorescence microscopy based on rylene dyes as a valuable tool for the characterization of materials.[98]

3.4. Nanoemitters for the Visualization of Polymerization Processes

In Section 3.3 we showed that rylene dyes can serve as sensitive reporters of motional as well as polarity changes in their immediate surroundings. We will now proceed from the molecular to the macromolecular level and introduce nanosized rylene emitters ("nanoemitters") as sensitive reporters. The covalent incorporation of chromophores into the core leads to macromolecular architectures of well-defined sizes.[43] The attachment of shape-persistent dendritic branches such as polyphenylenes to a central PDI dye substantially improves the film-forming properties, and the aggregation of PDI is efficiently suppressed in the solid state.[43] Adjusting the polyphenylene shell enables nanoemitters of well-defined size to be obtained. Figure 8 shows the transition from a molecular PDI emitter **13**, for example, bearing two reactive styryl groups, to a third-generation dendrimer **14** with a PDI dye in the center. An increase in the number of polyphenylene rings results in a stepwise augmentation of the sizes of the nanoemitters from 3.1 nm for the first-, 4.7 for the second-, and 6.1 for the third-generation dendrimers (Figure 8; PDI chromophores **15**, **16**, and **14**, respectively).

Since the diffusion coefficient reflects the capacity of a single nanoemitter to diffuse freely in a given environment, the ability to synthesize emitters of defined sizes allows the detection of changes in the surrounding nanoenvironment (for example, free volume or viscosity). For example, if the viscosity is increased, the larger macromolecules should be considerably more affected than single chromophores or smaller emitters. Such dendronized chromophores can, therefore, serve as efficient reporters of the viscosity or mobility of the direct surroundings.

SMS measurements were performed during the radical polymerization of polystyrene by detecting changes in the diffusion constants of rylene based dyes that were acting as probes.[44] A combination of fluorescence correlation spectroscopy (FCS) and wide-field single-molecule tracking (WFM) was used to collect these data. On the basis of the above-mentioned notion that the mobility of PDI reporter

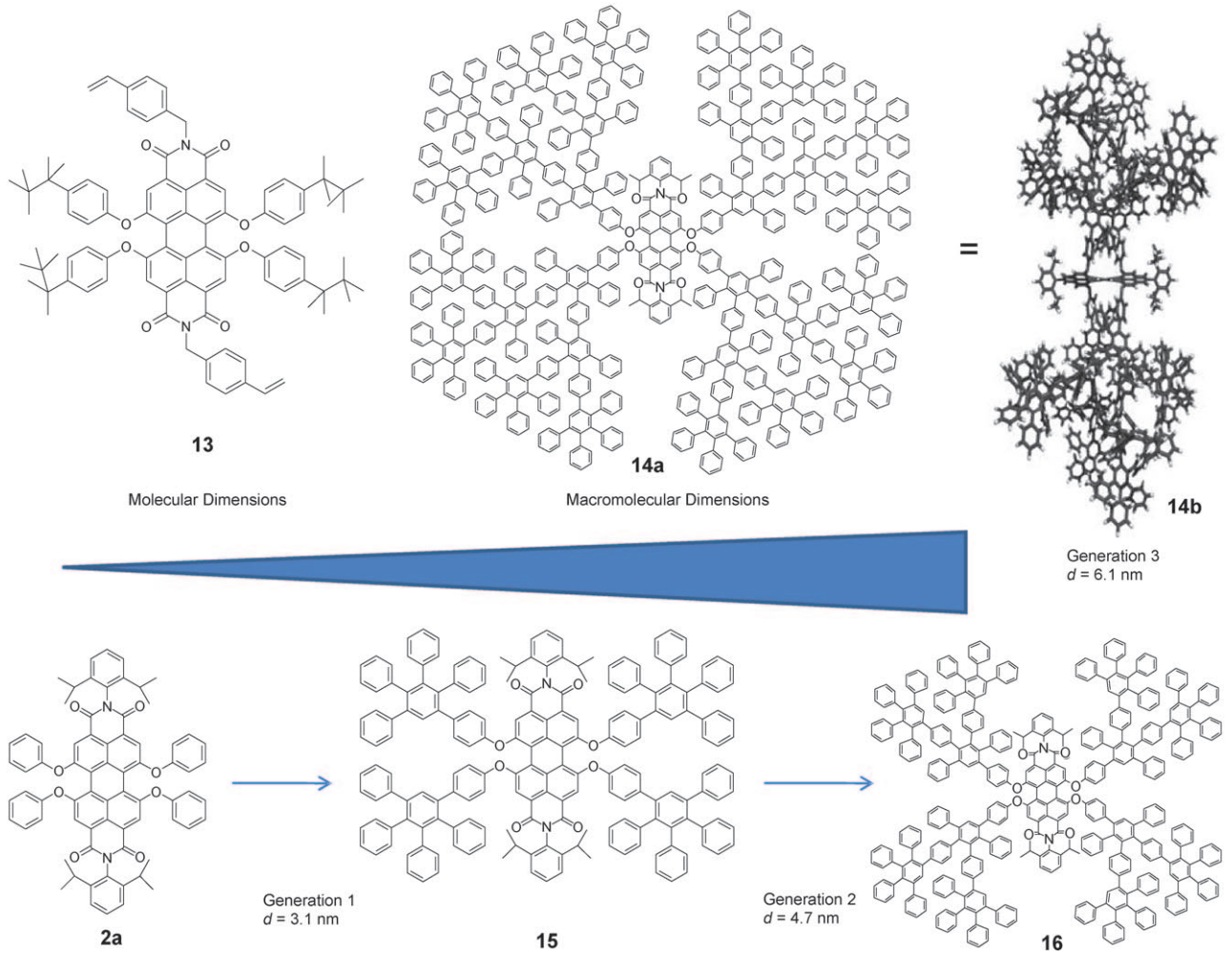

Figure 8. Two-dimensional structures of the molecular PDI emitter **13** with two reactive styryl groups that allow cross-linking through polymerization reactions. The transition from the emitter **2a** to the nanoscopic dendritic emitters **15** with four branches in the first generation, **16** with second-generation, and **14a** with third-generation polyphenylene dendrimer branches. **14a** has a 2D structure of a third-generation dendrimer with PDI in the center, while **14b** shows the 3D structure of the same molecule.

molecules changes during the polymerization process, variations in the diffusion times of molecular and macromolecular emitters were studied.

The dynamic ranges that can be covered by the two methods overlap, thus allowing the entire polymerization process to be monitored through fluorescence measurements. The polymerization of styrene in the absence and presence of a cross-linker was studied by using dye molecules **13** and **14a**.[44] In the absence of a cross-linker, **13** and **14a** diffuse freely in the surrounding medium, but, as expected, the more bulky molecule **14a** diffuses more slowly than the smaller molecules **13** or **2a** (Figure 9).[44] The rate of diffusion of both

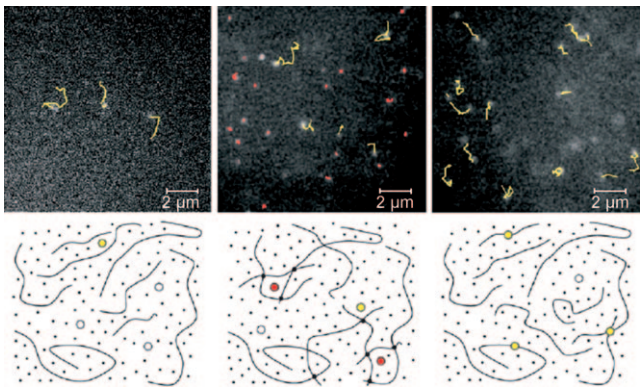

Figure 9. Top: WFM pictures at about 0.64 U (U is the conversion), including tracks for up to 20 steps for the three types of experiments discussed in the text. Left: **14a** without cross-linker. Middle: Dye **14a** with 1% cross-linker. Right: **13** without a cross-linker. Bottom: Schematic representation of the dyes in their surroundings. The dyes are shown as circles, the color of which indicates their current velocity (white: too fast for detection by WFM, yellow: slow enough for WFM, red: very slow/immobilized).

molecules decreases as a function of the conversion rate until the point is reached that FCS measurements are no longer adequate. From that point on, single molecules can be tracked by wide-field detection. In the presence of a cross-linker, the motion of the PDI reporter molecules describes the onset of heterogeneity, which arises during the formation of a network. This heterogeneity can be directly visualized during the wide-field measurements: a fraction of the molecules is clearly trapped by its nanoenvironment while the remainder seems to diffuse unhindered.

These investigations can be readily extended to other polymerization systems such as interpenetrating networks and nanocomposites. These studies will provide a deeper understanding of the factors that control heterogeneity in a polymerization process. Possible other applications include stimulated emission depletion microscopy (STEM), a technique that requires substantial photon loads on dye molecules[79,99–102], and catalysis,[103,104] in which the low level of intrinsic dynamics of some of the rylene dyes at the single-molecule level seems promising to follow the dynamics (individual turnover events) of the catalytic process itself.[105]

In Section 3 we showed that chemical modifications of the rylene chromophore core as well as changes in the dynamics or polarity of their direct environment have a considerable impact on their optical properties. In Section 4 we will introduce the concept of arranging distinct numbers of rylene chromophores in a restricted molecular volume. Such multichromophore nanoemitters offer the unique opportunity to study the result of varying the chromophore distance, orientation, and spectral overlap on energy-transfer processes on the single-molecule level.

4. Multichromophoric Nanoemitters and Energy Cascades

The concept of concentrating chromophores in a restricted volume has been perfected by nature in a variety of light-harvesting complexes,[106–108] and, to a certain extent, in multichromophore fluorescent proteins[109] such as the red fluorescent protein DsRed from *Discosoma* sp. The arrangement of multiple chromophores in proximity leads to interactions between the chromophores and influences their photophysical behavior. In particular, Förster-type energy-transfer processes (between identical or different types of chromophores) such as singlet–singlet energy transfer as well as singlet–triplet and singlet–singlet annihilation represent new and competitive excited-state deactivation pathways in multichromophoric systems.[58] Above, we described that individual rylene dyes are well-suited for single-molecule microscopy. Increasing the quantity of these bright emitters within one molecular scaffold offers additional features, such as considerably increased absorption cross-sections and high emission intensities, as well as prolonged observation and survival times. We will now discuss different design concepts for introducing multiple chromophores within a macromolecular scaffold. In this context, the impact of the size and shape of the scaffold, the orientation, distance, and nature of the chromophores on different energy-transfer processes will be highlighted. First, we will consider dendritic multichromophores where one type of rylene chromophore is placed at distinct locations in the scaffold of polyphenylene dendrimers. The molecular emitters obtained by this strategy are ideally suited to study energy hopping and singlet annihilation, and constitute a new class of "single photon on demand" emitters.[28,110–114] Next, we will discuss molecular and macromolecular dyads and triads containing different kinds of rylene chromophores. Such multichromophores allow in-depth investigations of excited-state energy-transfer processes on the single-molecule level, which allow a better understanding of nature's light-harvesting arrays.

4.1. Dendritic Nanoemitters.

Dendrimers are monodisperse, repeatedly branched cascade molecules with a very high spatial order.[115] Polyphenylene dendrimers, which consist of benzene units as building blocks, are considered as rigid, monodisperse, and shape-persistent macromolecules.[116,117] They offer access to complex macromolecular structures with an extremely high degree of structural organization and the possibility to

introduce chromophores in the core (see Figure 8 in Section 3.4), within the dendritic scaffold, or at the periphery.[118] Besides the topologically defined location of the functional groups and the high shape persistence, a further advantage of polyphenylene dendrimers for use as a nanosupport is the absence of functional groups within the dendritic scaffold. This makes them chemically and thermally highly stable. In addition, the opportunity to modify the substitution pattern of rylene chromophores as well as the scaffold of polyphenylene dendrimers allows for the precise adjustment of chromophore distances and orientations within a defined nanoscopic volume. Furthermore, polyphenylene dendrimers are optically inert in the visible part of the spectrum, for example, because of the presence of twisted benzene rings. Polyphenylene dendrimers absorb at up to 350 nm, depending on the generation considered, and do not emit above 450 nm.[119] Therefore, they represent an ideal scaffold since they do not interfere with energy-transfer processes themselves, provided that the chromophores involved are chosen to absorb and emit in the visible part of the spectrum.[118,120]

A biphenyl unit **19**[121–123] or a tetraphenylmethane moiety **17** or **18**[28,124–129] were chosen as central dendrimer cores for the preparation of polyphenylene dendrimers with different numbers of PMI chromophores at distinct locations of the periphery (Figure 10). The tetraphenylmethane core ensures a higher structural rigidity as well as the formation of a globular architecture, whereas the biphenyl unit results in a higher degree of mobility along the biphenyl unit as well as a flatter architecture.[121,130] Symmetric polyphenylene dendrimers of the first, second, and third generation based on a tetraphenylmethane contain 4, 8, and 16 PMI chromophores at the periphery, respectively, whereas functionalization of dendrimers with a biphenyl core resulted in a higher PMI density of 8, 16, and 32 PMI chromophores for the first, second, and third generation of the dendrimer, respectively.[121]

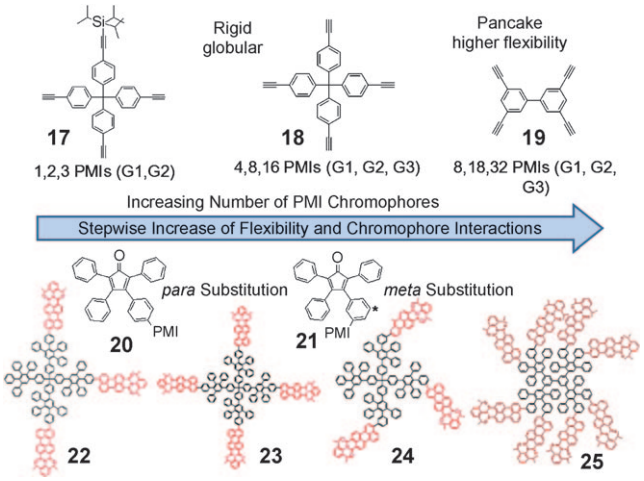

Figure 10. Overview of the design concepts for achieving dendritic multichromophores with various numbers of PMI chromophores, predefined geometries, different chromophore orientations, and various chromophore distances. The terms "1, 2, 3 PMIs" refers to dendrimers with one, two, or three PMI chromophores at the periphery. G1–G3 denote the dendrimer generation. *: refers to the attachment point.

In addition to the dendrimer core, the number of PMI chromophores within one dendrimer generation was varied systematically.[130] The consecutive growth of single dendritic branches from the desymmetrized tetraphenylmethane core **17** was achieved by a convergent approach (synthesis of the dendrons first and then reaction with the core molecule). In this way, first-generation polyphenylene dendrimers with an increasing number of (one to four) PMI chromophores were obtained. For example, 3 PMI dyes (in the case of **22** and **24**) could be exclusively located at the periphery of dendrimers with diameters of approximately 3 nm.[130] In the case of second-generation dendrimers, single dendrimers with precisely one to four chromophores were obtained. Calculations on energy-minimized structures suggest diameters of about 5 nm (Figure 11). In addition to the number, the orientation of the chromophores was varied by attaching the PMI chromophores in the *meta* (**24**, **25**) or *para* positions (**22**, **23**) of the outer phenyl groups of the dendritic scaffold.

4.2. Photophysical Properties of Dendrimer-Based Multichromophores

The Förster model is applicable when two fluorescent chromophores are in proximity (2–10 nm range) and there is a weak interaction between their transition dipole moments.[132] The physical basis for this so-called Förster resonance energy transfer (FRET) involves the transfer of excitation energy from a donor to an acceptor with two weakly coupled transition dipole moments. The process is best known for dedicated donor and acceptor molecules; however, the original theory was derived for a system in which the acceptor was chemically identical to the donor molecule. This phenomenon is now commonly known as energy hopping or homo-FRET.[126,133]

Within the Förster model, direct excitation of one of the PMI chromophores in a multichromophoric dendrimer can lead to energy hopping to a neighboring chromophore. The distance (R_0) at which there is a 50 percent change in this process is called the Förster radius, and can be calculated from Equation (1). In this Equation, κ^2 represents the an

$$R_0 = 0.211(\kappa^2 n^{-4} \Phi_D J(\lambda))^{1/6} \quad (1)$$

orientation factor, which describes how the transition dipole moments are oriented, n is the refractive index of the medium, Φ_D is the quantum yield of the donor, and $J(\lambda)$ is the spectral overlap of the emission spectrum of the donor with the absorption spectrum of the acceptor. For nonparallel oriented chromophores, energy hopping can be determined experimentally by time-resolved fluorescence depolarization experiments. Depolarization measurements were carried out on a series of four first-generation polyphenylene dendrimers based on a tetraphenyl core with increasing numbers of one up to four PMI chromophores attached at the *meta* position (for example, **24** of Figure 12 with 3 PMI chromophores).[134] Besides the rotational correlation time of the chromophore,

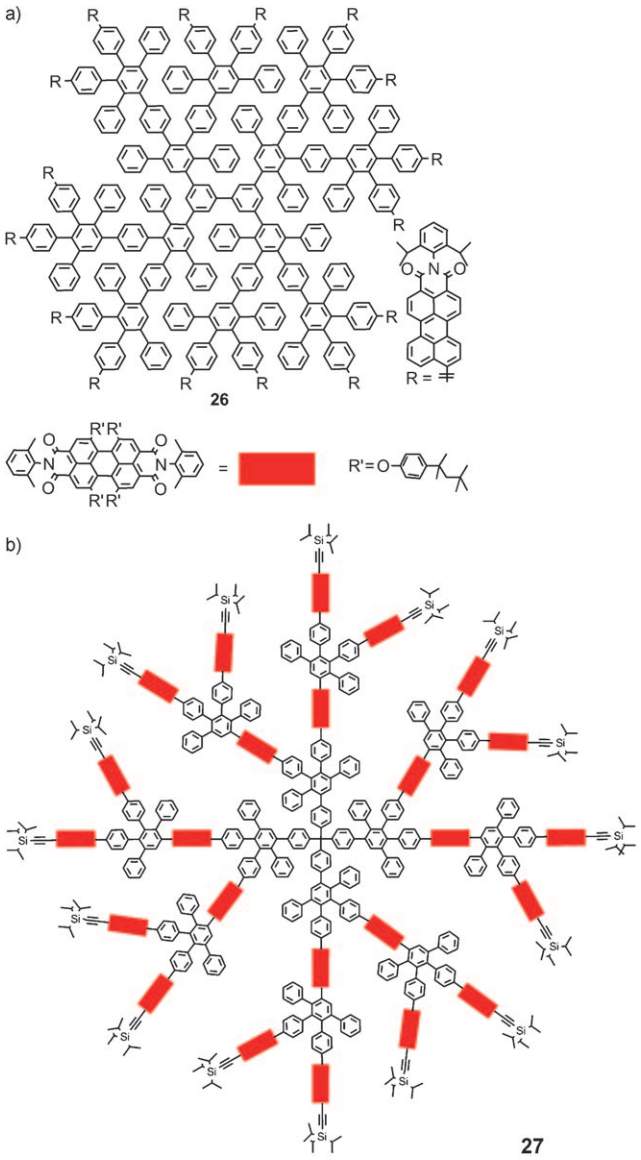

Figure 11. a) Second-generation dendritic multichromophore **26** based on a biphenyl core with 16 PMI dyes at the periphery. The terminal, protected ethynyl groups allow for further growth of the dendrimer. The generation of perfectly defined arrangements of multichomophores was achieved by using this design concept. Higher dendrimer generations, such as **26**, were prepared with 16 PDI chromaphores (second generation) as well as 32 dye chomaphores (third generation). b) In an another approach, a desymmetrized PDI dye was used as a branching reagent to generate second-generation dendrimer **27** with a larger molecular diameter (up to 12 nm) and up to 24 emitters in the dendrimer scaffold.[131] By applying the synthesis concepts described in Section 4.1 highly fluorescent nanoemitters with an extremely high number of dye molecules were prepared, which had a defined volume and whose density of dye molecules was comparable to the natural light-harvesting complex. The photophysical properties of multichromophore dendrimers are discussed in Section 4.2.[131]

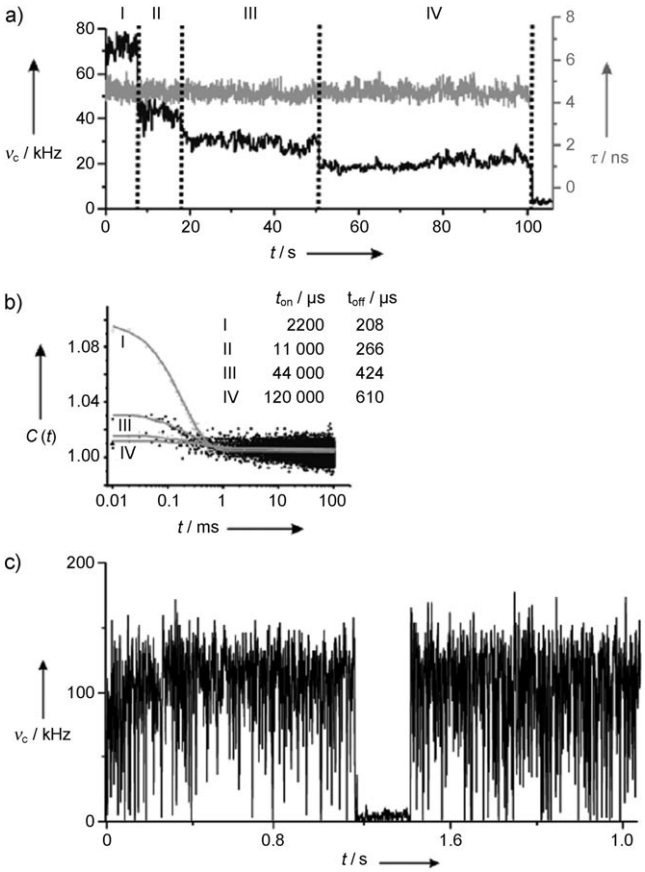

Figure 12. a) Fluorescence intensity (count rate ν_c [kHz] versus time t [s]) and fluorescence lifetime trajectory (fluorescence lifetime τ [ns] versus time t [s]) of a single molecule of dye **23**. b) Second-order intensity correlation of the different intensity levels clearly demonstrates different "off" times (triplet related) at different intensity levels. c) Expanded view of the first intensity level of a single molecule of **23**, which demonstrates short "off" times (triplet related) and one long "off" event (related to formation of an anion).

an energy-hopping component was found that could be correlated to the increasing number of PMI chromophores.

Two excited states (S_1) can be present in a single molecule at the same time if the multichromophoric system undergoes optical excitation under high photon flux. If the $S_1 \rightarrow S_0$ transition of one chromophore is in resonance with a transition of the other chromophore from S_1 to a higher excited singlet states, that is, a $S_1 \rightarrow S_n$ transition, energy transfer between the excited singlet states can occur. The process results in only one excited state remaining in the multichromophoric system and is often referred to as singlet–singlet annihilation.

The presence of this process was already proven at the ensemble level by means of femtosecond fluorescence upconversion and time-resolved polychromatic femtosecond transient absorption measurements.[135] At the single-molecule level, singlet–singlet annihilation ensures that multichromophoric dendrimer systems act as excellent single photon sources. Indeed, increasing the number of chromophores at the nanometer scale results in a higher absorption cross-section. Multiple excitations can be generated with each pulse if pulsed laser light is used (higher excitation powers), just like in solution. In the case of efficient singlet–singlet annihilation, which depends on the spectral characteristics of the chromophores used and the distance between them, the

process represents a feedback mechanism that ensures the emission of only one photon per pulse, even though multiple excitations have occurred. The application and quality of several of the structures discussed in Section 4.1 as single-photon sources have already been investigated and quantified.[28,126,127,129,136–138] Other approaches to generate single-photon sources with dendronized rylene systems comprise shockwave-induced particle formation with compound **16**, in which aggregation of the chromophores is prevented, and tightly packed particles with large cross-sections are produced.[45,46]

Repeated excitation (as in the case of single-molecule studies) of the chromophores can also lead to ISC to the triplet state. The relatively long lifetime of the triplet state means that a second chromophore in the individual dendrimer molecule can be excited while the first chromophore is still in the triplet state. As a result, two excited states are present, a S_1 and a T_1 state. If the triplet state undergoes transitions into higher excited triplet states, T_n, that are in resonance with the $S_1 \rightarrow S_0$ transition, energy transfer from the excited singlet state to the energetically lower-lying triplet state, can occur.[126] This process is often called singlet–triplet annihilation. Such a process is not easy to see in bulk experiments, but manifests itself directly in single-molecule fluorescence trajectories as collective "on/off" steps (see Figure 12a).[126] Careful analysis of the "on/off" jumps that correspond to different intensity levels in multichromophoric systems can result in quantitative information on ISC, and even ISC involving higher excited states (see Figure 12b).[129]

Besides the above-mentioned on/off blinking process, there is an additional rarer event that leads to longer fluorescence intermittence than excursion to the triplet state. Long off times (in the range of seconds) are caused by the formation of a radical anion on one of the rylene chromophores. This radical anion can quench the fluorescence of the other chromophores through energy transfer (see Figure 12c).

4.3. Light Harvesting and Energy Cascade Systems.

In Section 4.1 design concepts for the introduction of either PMI or PDI chromophores into the core, the scaffold, or the periphery of polyphenylene dendrimers were described. This concept was extended to the attachment of different rylene dyes, for example, naphthaleneimide, PMI, and TDI chromophores, to generate light-harvesting arrays for the vectorial transfer of excitation energy.[124,139] Nature has perfected this principle, as can be seen from the crystal structure of the light-harvesting antenna complex (LH2) of the purple bacterium *Rhodopseudomonas acidophila*.[140] In biological systems, a combination of Förster-type energy transfer and strongly coupled chromophores arrays is used to transfer energy over large distances.[141,142] Additionally, the chromophore systems are protected from photobleaching by the presence of other molecules, for example, carotenoids.[143–145] The introduction of strong and weak coupling as well as protective units in one molecular system is at present out of reach for synthetic chemistry and, therefore, we focused first on achieving a cascade of energy transfer by spatially arranging arrays of FRET-donor and FRET-acceptor molecules.

In a photosynthetic system, light is generally collected by the antenna system and transferred to the reaction center. Thus, chromophores absorbing at short wavelengths are located at the outside and transfer their energy to acceptor chromophores that absorb at longer wavelengths. Thus, we arranged different rylene dyes in a similar fashion on a dendritic scaffold. PMI, PDI, and TDI chromophores are excellent chromophores for investigating directed energy-transfer processes because of their fairly large absorption cross-sections and high emission quantum yields. The rigidity of the scaffold is of paramount importance to maintain precise interchromophore distances and allow quantitative interpretation of the obtained data. Many other dendrimer-based vectorial energy transfer systems have been proposed in which the lack of structural rigidity hampered quantitative interpretation.[146,147]

Bichromophoric molecules, that is, donor–acceptor (D/A) dyads composed of a designated PDI donor molecule and a designated TDI acceptor molecule linked by fairly rigid oligophenylene spacers with different lengths,[148,149] have been designed as model systems for the more complex dendrimers. The term "dyad" corresponds to a bi- or multi-chromophore that bears two different types of chromophores. At the same time, the influence of the orientation of the chromophores on the energy-transfer process can be nicely demonstrated (Figure 13).[148,149]

The geometry of linear-chain macromolecules is not ideal for efficient energy transfer; in particular, it is difficult to achieve an energy gradient for a vectorial transduction of light energy over long distances.[150] Nevertheless, a system comprising a rigid DNA scaffold and five different dyes resulted in energy transfer over 13.6 nm and covered a spectral range of 200 nm.[151,152] However, in our view, and inspired by the geometrical arrangements found in natural light-harvesting systems, the globular shape of dendrimers has the distinct advantage that it provides a large surface area that can be decorated with multiple chromophores.[153] Globular dendritic light-harvesting arrays were designed according to two different kinds of strategies: The first approach comprised the localization of the shorter-wavelength-absorbing PMI chromophores as well as the longer-wavelength-absorbing TDI dye at the periphery of a first-generation polyphenylene dendrimer (Figure 13a). In a second attempt, the TDI chromphore was placed at the center of a dendrimer, surrounded by four or eight terminal PMI chromophores (Figure 13b,c). **28**–**30** represent three molecular PMI–TDI dyads corresponding to the two design concepts. Dyad **28** with three PMIs and one TDI chromophore was generated by a convergent-growth approach, which facilitated an asymmetrical distribution of functional groups at the periphery. Such a well-defined distribution of substituents is based on a "desymmetrization" step as the synthetic key step by using a nonsymmetric tetraphenylmethane core such as **17**. This dyad behaves as a light-harvesting antenna, since a directed energy transfer occurs from the PMI chromophores toward the TDI dye.[43,48,124,125,130,134,154,155]

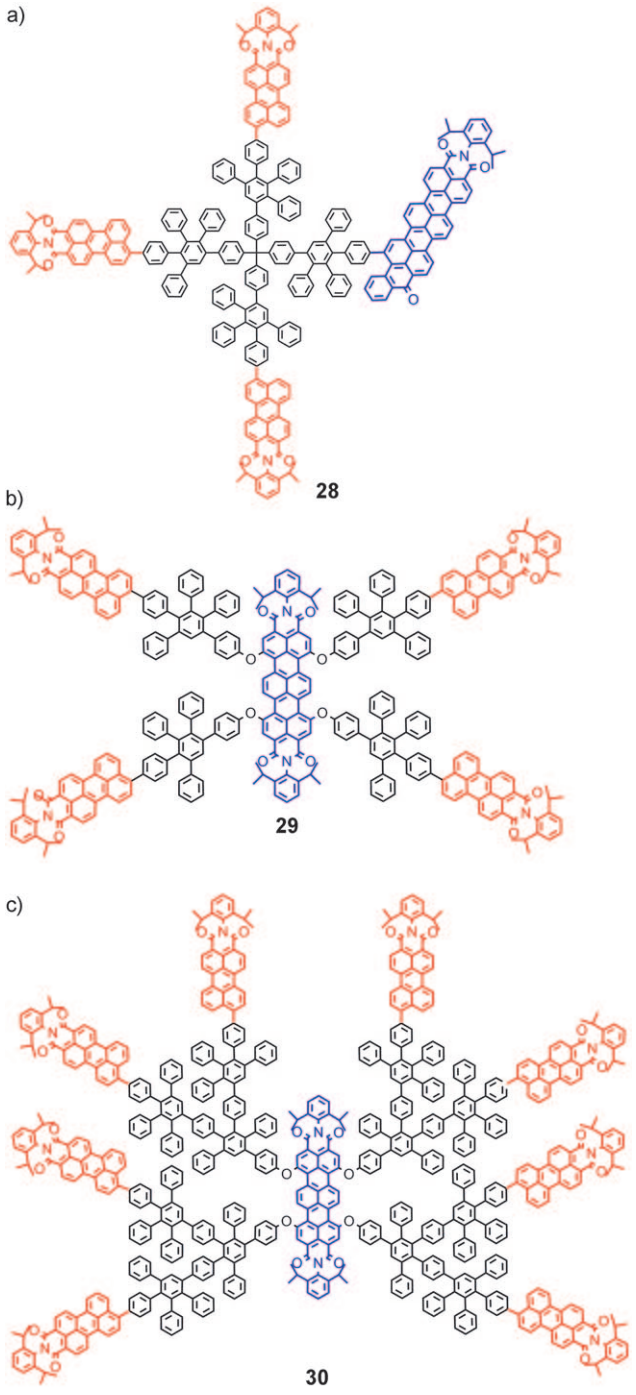

Figure 13. a) Dendritic dyad **28** with 3 PMI chromaphores and one TDI chromophore at the periphery. b) First- and c) second-generation polyphenylene dendrimers **29** and **30** with a TDI chromophore in the center and 4 and 8 PMI chromophores, respectively, at the periphery.

In contrast to **28**, dendritic dyads **29** and **30** with the TDI chromophore in the center and PMI chromophores at the periphery revealed a high photostability that is suitable for single-molecule experiments. An efficient, vectorial energy transfer through an energy gradient from the periphery towards the center of the dendrimer was obtained for multichromophores based on this design concept. For **29**, it was found by two-color (separate donor and acceptor channels) experiments that the bleaching of PMI chromophores can compete with the nearly quantitative energy transfer between PMI and TDI. This suggests that bleaching can also occur from the singlet state of a molecule.[156] Simultaneous emission in the donor and acceptor channels was detected at later stages in the fluorescence trajectories of individual molecules of **29** and **30**. A detailed defocused wide-field study revealed that unfavorably oriented donor molecules (with respect to the acceptor) are responsible for the observed simultaneous emission, rather than an exciton blockade.[9,157]

Probably the most elaborate architecture devised for vectorial energy transfer is the third-generation globular polyphenylene dendrimer **31** (Figure 14) with a TDI chromophore as a core, PMI chromophores in the scaffold, and NMI chromophores at the peripherty. This nanoemitter reveals a high degree of complexity since all the spatial locations, distances between the chromophores, and their absorption and emission spectra were adjusted carefully.[158] In this way, an efficient dendritic triad was obtained that absorbs light over the whole spectrum of visible light and shows stepwise energy transfer over long distances from the periphery via the scaffold towards the center of the dendrimer.

Such multichromophores show a similar structural complexity as natural light-harvesting arrays.[51,158] A single-molecule study revealed that there is a competition between the cascade transfer NMI-PMI-TDI and directional transfer between the NMI-TDI chromophores, most probably as a consequence of spectral overlap of the emission spectrum of NMI and the $S_0 \rightarrow S_2$ absorption band of TDI.[51]

In natural arrangements, the antenna system is coupled to a redox center in which electron transfer occurs. Coupling an antenna to a redox center is a clever design that offers multiple advantages: 1) the cross-section is increased, thus the probability that a photon is captured by the antenna is much larger than if the reaction center was directly excited. This ensures that reaction centers can be cycled much more rapidly. 2) The antenna displays a broader absorption spectrum than the reaction center, thus photons of various energies can induce the electron-transfer reaction. A next logical step is to combine the antenna systems we designed with an artificial type of reaction center to induce electron transfer. Usually electron-transfer reactions are fast, on the order of picoseconds, and, as a result, fluorescence is quenched. Ultrafast pump-probe measurements are often used to follow or deduce the kinetics of electron-transfer reactions in bulk measurements. At the single-molecule level it is much harder to study electron transfer for the simple reason that fluorescence is quenched.

5. Redox-Active Chromophore and Multichromophore Arrangements

5.1. Electron Transfer in Rylene Compounds

Electron transfer (ET) involves a pair of electron-donor and electron-acceptor entities, and its efficiency decreases

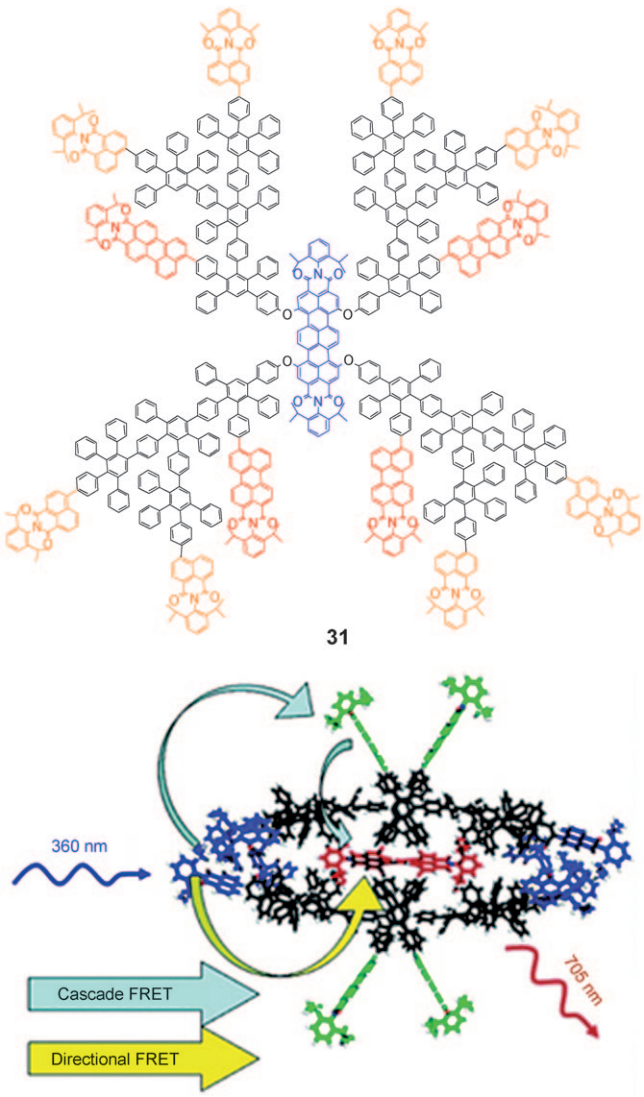

Figure 14. Top: Chemical structure of the triad **31** containing eight NMI chromophores in the outer shell, four PMI chromophores within the scaffold, and one TDI in the center. Bottom: The arrows in the 3D structure of **31** illustrate energy-transfer processes after exciting the NMI chromophores.

exponentially with increasing donor–acceptor distance. However, whereas a highly efficient FRET results in fluorescence emitted mainly from the acceptor chromorophore, a highly efficient ET usually leads to a strong quenching of the fluorescence of the emitting chromophore. At the bulk level, systems based on rylene dyes have been reported in which electron transfer was studied by fast spectroscopic techniques.[159,160] In contrast to single-molecule FRET investigations, studies dealing with single-molecule-photoinduced ET (ET that occurs when the donor is in the excited state as a result of the absorption of a photon) are rather limited because of the occurrence of the strong quenching mentioned in Section 4.3.

One of the few reports published on electron transfer at the single-molecule level employed PDI, which was separated from an indium tin oxide (ITO) electrode by a self-assembled monolayer (SAM; Figure 15a). The SAM prevents direct

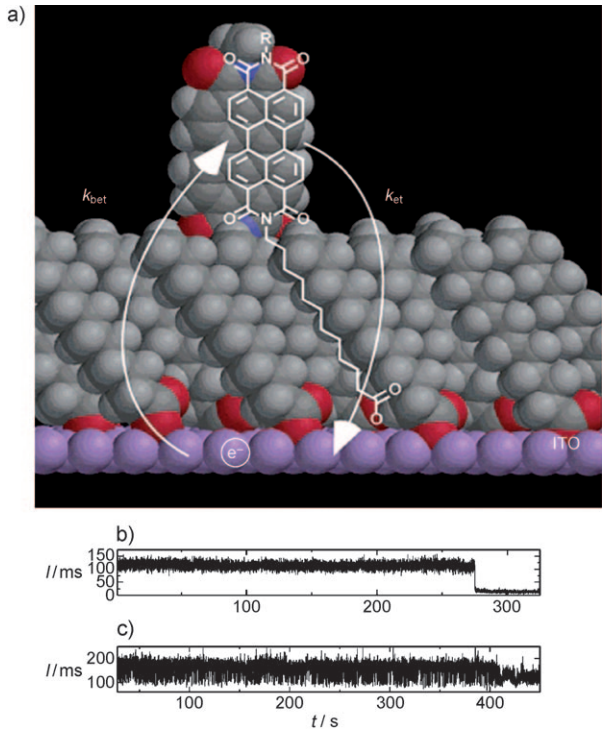

Figure 15. a) Schematic representation of an interfacial electron-transfer system based on a PDI chromophore with an carboxylic acid alkyl tail that is self-assembled in a mixed monolayer on an ITO electrode (R = 1-hexylheptyl). b) Fluorescence trajectories (counts in 20 ms) for a PDI chromophore on quartz and c) in a self-assembled monolayer on ITO. At $t = 275$ s, an irreversible photobleaching of the PDI chromophore occurs.

contact between the PDI and the electrode surface, therefore slowing the ET process between the photoexcited PDI and the electrode such that fluorescence can still be observed. As indicated in Section 3, PDI chromophores studied at the single-molecule level usually show very few long blinking events, as exemplified in Figure 15b for PDI on quartz. Bringing PDI chromophores in close contact to an ITO electrode leads to a drastic increase in the amount of blinking that is observed, as can be seen in Figure 15c for a SAM in which a PDI chromophore is randomly incorporated.[161] Since the occurrence of the longer (more than 20 ms) off times is clearly related to the proximity of the ITO electrode, it is deduced that these blinking events result from electron transfer to the ITO electrode. Further studies based on this concept should lead to a better understanding of the effect of the length and nature (conjugated versus nonconjugated) of the spacer and of binding functional groups on the rate of electron transfer. This question is of enormous interest to both molecular electron transfer experimentalists and theoreticians.

A special case of ET is the case when the locally excited state (LES) and the charge-separated state (CSS) are close in energy. Upon excitation, the LES deactivates mainly by forward ET to the CSS and, if the radiationless deactivation of the CSS to the ground state (GS) is inefficient (Figure 16), the CSS decays via the LES by reverse ET. As a net result, the emitted fluorescence is delayed but can retain a high quantum yield.[162–164]

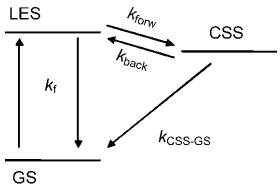

Figure 16. Forward and back electron transfer resulting in delayed fluorescence. LES = local excited state, GS = ground state, CSS = charge-separated state, k_{forw} = rate constant for the forward electron transfer, k_{back} = rate constant for the back electron transfer, k_{CSS-GS} = rate constant from the charge-separated state to the ground state.

To explore photoinduced electron transfer by fluorescence we designed dendritic architectures based on the building-block concept described in Section 4, which allows electron-donating and electron-accepting groups to be introduced at the center as well as at the periphery of a polyphenylene dendrimer.[165] In view of the exponential distance-dependence of the ET process, the structural rigidity provided by the polyphenylene units represents a key feature to control the distance between the donor and acceptor moieties. In this way, molecular dyads were prepared that consisted of electron donors covalently linked through polyphenylene spacers to a PDI chromophore, which acts as an acceptor.[165] Redox-active triphenylamine (TPA) groups, which are widely used as hole-transport (HT) and electron-donor materials,[166,167] were introduced into the *bay* region of PDI (Figure 17).[165] The distance between the PDI electron acceptor and the TPA donors was varied at the nanoscale by increasing the number of dendrimer generations. This design concept further benefits from the presence of the rigid dendritic shell, as electronic coupling between the PDI and TPA substituents is increased and self-quenching caused by aggregation of PDI[43] is suppressed.

Single molecules of **32**–**34** were embedded in polystyrene. As intended, individual donor–acceptor molecules undergo reversible electron transfer, as can be deduced from the delayed fluorescence that is emitted with a high photon count rate.[164] Fluctuations in both the forward and backward electron transfer spanning a broad range, from milliseconds to seconds, were found by monitoring the fluorescence decay times. The observed fluctuations were shown to be induced, on the one hand, by conformational changes in the dendrimer structure and, on the other hand, by reorientations of the polymer chain in the vicinity of the observed single molecules. Conformational changes have been linked to libration, that is, changes in the torsional angle of adjacent phenyl rings located in the dendritic branches near the donor moiety that transfers the charge. The net result of this torsional motion is a change in the through-bond donor–acceptor coupling, which induces fluctuations in the decay time on the millisecond time scale. Reorientation of the polymer chain resulted in changes in the local polarity of the donors and hence to changes in the solvation of the CSS.

Up until now, material-science-related applications of rylene dyes have been discussed. More specifically, the environments in which the rylene derivatives were used turned out to be highly apolar. This fits well with the large aromatic moieties that comprise this class of colorants. A key question is whether the superior performance of rylene dyes can also be exploited in aqueous environments, notably in biological applications. This question will be addressed in the next section.

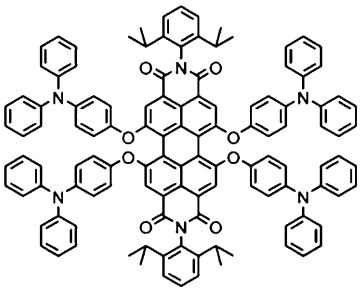

32

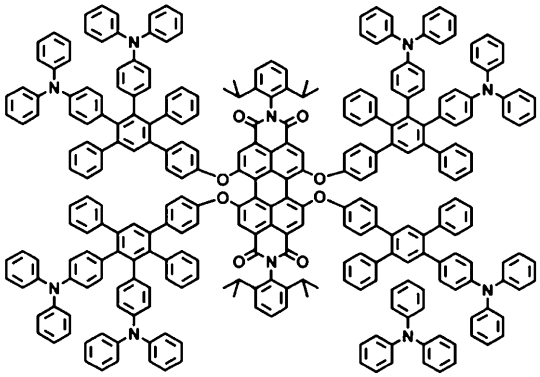

33

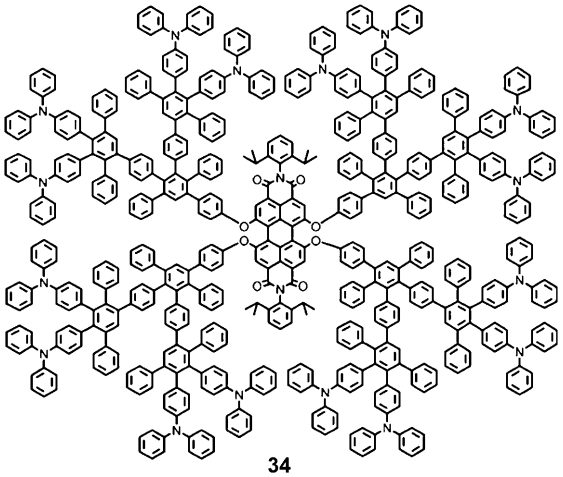

34

Figure 17. First-, second-, and third-generation polyphenylene dendrimers (**32**, **33**, and **34**) based on a PDI core with 4, 8, and 16 TPA groups at the periphery, respectively.

6. Applications of Rylene Dyes in Biogical Systems

6.1. Water Solubility

Fluorescence techniques are well-suited to investigate many fundamental biological processes such as the interplay

or trafficking of biomolecules.[8] A suitable biolabel 1) can be excited without exciting the biological matrix, 2) is soluble in relevant buffers, 3) is biocompatible, 4) has a high molar extinction coefficient, 5) has a high fluorescence quantum yield, as well as 6) having a single functional group for site-specific labeling.[8] Rylene dyes have mainly been used for applications in organic solvents because of their highly lipophilic nature and their strong tendency to form aggregates in a polar environment. As a consequence of their extended aromatic scaffolds, rylene chromophores are not soluble in water and the introduction of water-solubilizing groups while preserving a high fluorescence quantum yield has been a challenging goal.[42] Perylene chromophores carrying hydrophilic substituents, such as sulfonic acid moieties[42,168] and quaternized amine groups[42] or crown ethers, polyethylene oxide,[169,170] or peptide chains[170] attached to the chromophore showed almost no fluorescence in water.[42] For example, in the case of a PMI chromophore with a long PEO tail (PMI-PEO), the loss of fluorescence was directly connected to the formation of aggregates in polar solvents.[169] The presence of the long PEO chain results in this chromophore showing good solubility in polar and apolar solvents. Interestingly, the fluorescence quantum yields of this chromophore reflected the polarity of the surrounding media. In a hydrophobic environment, high fluorescence quantum yields were found, whereas in polar solvents, the fluorescence quantum yields dropped significantly because of aggregate formation. In this way, PMI-PEO served as a nanoreporter for polarity changes in its direct vicinity, a feature that was exploited in cell-staining experiments. Its bright emission in a hydrophobic environment as well as its low fluorescence quantum yields in aqueous media has resulted in this PMI-PEO nanoemitter being used to selectively stain cell membranes in in vitro experiments.[10,19] This feature was further exploited for a PMI derivative with a single carboxylic acid group (**35**, PMI-COOH,[169] see Figure 18a). This amphiphilic molecule was designed to interact with membranes. The planar aromatic scaffold of PMI has a high driving force to intercalate into lipid layers, whereas the carboxylic acid group was designed to mimic the negatively charged phosphate groups at the membrane surface. **35** has an extinction coefficient of 38000 $M^{-1}cm^{-1}$ at 500 nm and nearly quantitative fluorescence quantum yields in organic solvents. However, **35** is practically devoid of fluorescence in water, because of the formation of aggregates in polar solvents that are characterized by red-shifted emission bands, strongly reduced fluorescence quantum yields, and a longer decay time compared with the PMI monomer.[123] Furthermore, it was demonstrated that the photostability and hence survival time of **35** in a membrane is much higher than those of commercially available membrane dyes.[171] When **35** is added to a medium of growing cells, the dye stains the membrane, thereby rendering the cells brightly fluorescent. It was demonstrated by using giant unilamelar vesicles with different compositions as model systems for cells that the decay time of incorporated **35** strongly depends on the phase (fluid phase versus liquid-crystalline phase) of the phospholipids used.[171] This observation could be explained by differences in packing, and in the free volume between

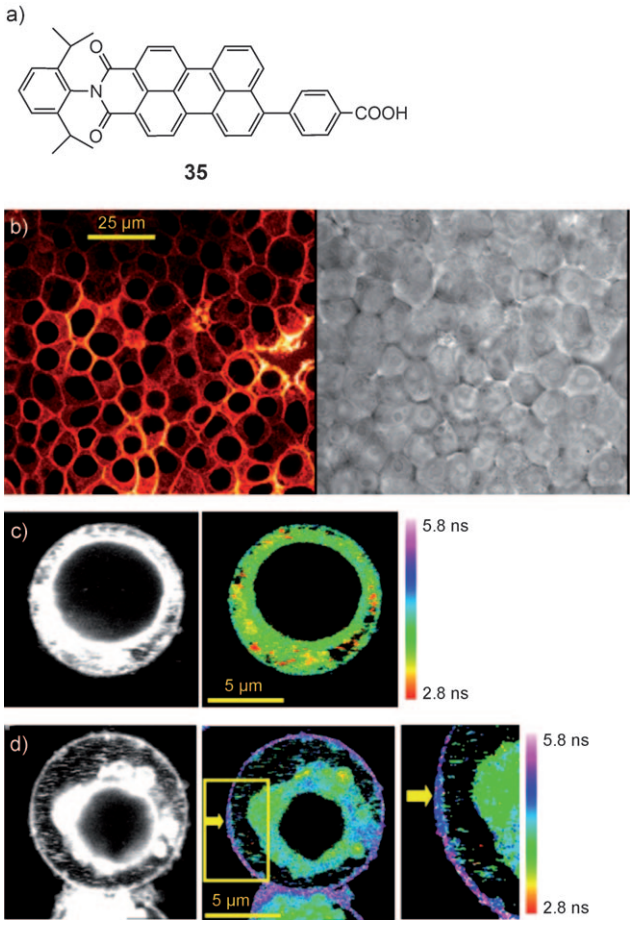

Figure 18. a) Structure of the amphiphilic PMI-COOH dye **35**. b) Fluorescence (left) and transmission image (right) of HeLa cells on a coverslip treated with **35**. c) Fluorescence intensity (gray) and fluorescence lifetime images (color) obtained for **35** in a Jurkat cell after extraction of the cholesterol with methyl-β-cyclodextrin. d) Fluorescence intensity (gray) and fluorescence lifetime images (color) obtained for **35** in a Jurkat cell stimulated by cross-linking membrane CD3 receptors by using specific antibodies (4 μL mouse anti-CD3 antibodies (Sigma)); the yellow arrow points to a region where the lifetime of **35** is different from that in the rest of the membrane. This result is attributed to the formation of a large lipid raft. All FLIM images are represented using the same scale bar, from 2.8 to 5.8 ns.

different phases.[171,172] The sensitivity of the lifetime of the dye to its local environment suggests that it could be used to probe the local packing in cell membranes, notably in studies on lipid rafts, in combination with fluorescence lifetime imaging (FLIM). Lipid rafts are microdomains rich in cholesterol that are thought to exist in cell membranes and they are believed to play an important role in signal transduction. Figure 18c,d shows intensity images (gray) and lifetime images of Jurkat cells stained with **35**. Figure 18c shows images of a cholesterol-depleted cell, whereas Figure 18d shows images of a cell in which the formation of large rafts was induced. According to the lifetime images, clear differences in the decay times between the two cells and even within parts of a cell (enlarged image right in Figure 18d) were elucidated. This experiment validates the use of rylene dyes in biological research and stimulated us to explore more

advanced strategies of attaching polar substituents to the rylene scaffold.

The most successful approach for achieving water solubility and a high quantum yield of fluorescence is based on the introduction of hydrophilic substituents into the *bay* region of the chromophore.[173] In particular, PDI derivatives with four sulfonic acid (**36**), pyridinium (**37**), or quaternary amino groups displayed good spectroscopic properties.[42] Interestingly, in contrast to PDI, the TDI analogue with four sulfonic acid groups in the *bay* region revealed a high tendency to form nonfluorescent aggregates in water.[10,19] This dye also showed a high affinity to lipophilic environments and a high photostability, which was explored for the fluorescence labeling of lipid membranes and membranes containing compartments such as artificial liposomes or endosomes in living HeLa cells (Figure 19).[10,19]

Rylene emitters exhibit superior properties compared with most other dyes in single-molecule experiments, particularly when embedded in polymer films. In this context, a single-molecule study of **36** in polymeric films revealed excellent photostability with respect to photobleaching, far above the photostability of other common water-soluble dyes, such as oxazine 1, sulforhodamine B, and a water-soluble perylenediimide derivative.[10,19] A new type of chromophore was introduced recently to the WS-TDI family. WS-TDI pyridoxy **37** is the first analogue reported that does not form aggregates and thus fluoresces in water, while its photophysical properties are preserved.[19] The strategy of introducing charged substituents into the *bay* region of rylene chromophores represents the structural basis for the application of rylene dyes as biolabels, which is elaborated in more detail in Section 6.2.

6.2. Monofunctional Perylene Dyes for Protein Tagging

Chemical and biological labeling is essential for the exploration of protein function since fluorescent probes allow the detection of molecular interactions, mobility, and conformational changes.[174] In particular, FRET has become an important tool to study the conformational distributions and dynamics of biomacromolecules.[175] Such studies, however, require the ability to introduce fluorescent reporters at specific sites of the protein.

There are currently a variety of chromophores to choose from. Organic dyes, metal–ligand complexes, lanthanide chelates, and fluorophores of biological origin such as phycobiliproteins or genetically encoded proteins as well as nanocrystal chromophores have been applied successfully as biolabels.[8] Fluorescent probes such as bodipy,[6] Alexa,[176] and ATTO[177] derivatives combine high fluorescence quantum yields, moderate to good solubility, as well as low nonspecific adsorption. These dyes have been used, in particular, for experiments in a polar environment, such as water, buffers, or cytoplasm, and have been applied to a broad range of applications including SMS.[178] Until now, rylene dyes have been less popular for labeling biomolecules in aqueous solution, even though remarkable progress in designing improved PDI and TDI probes has been achieved recently by tailored functionalization approaches (Figure 20).

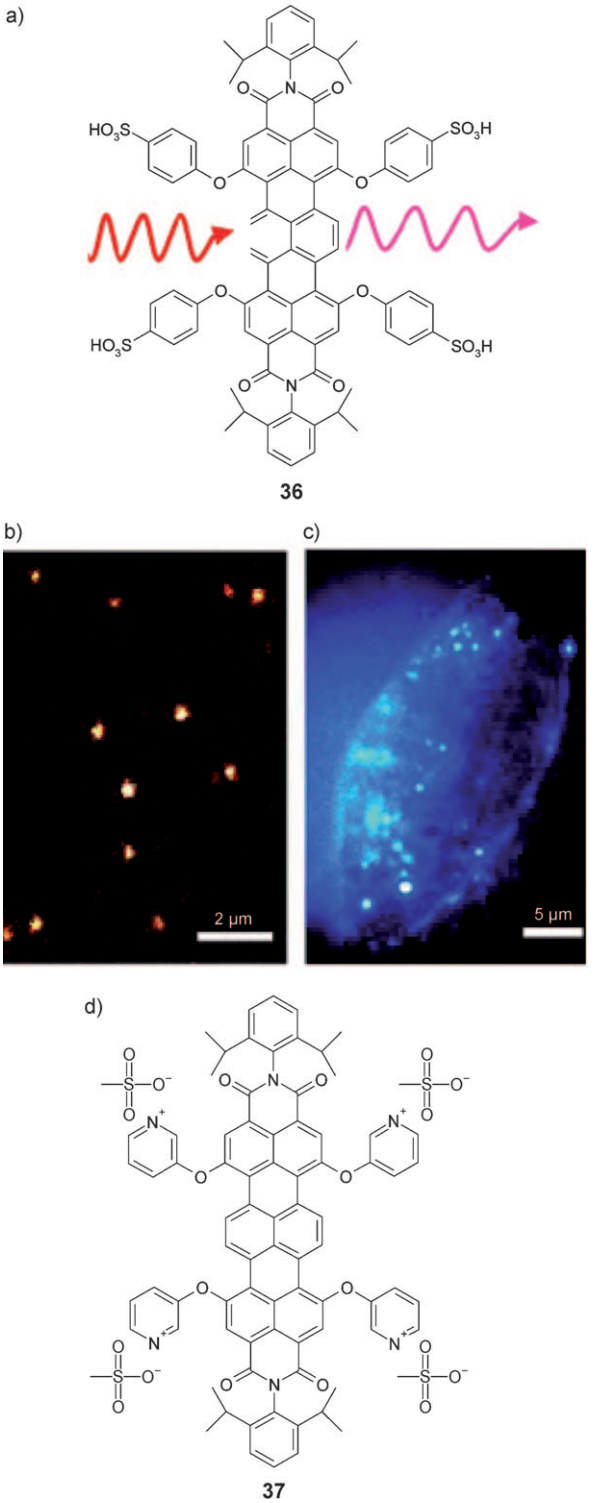

Figure 19. a) Structural formula of **36**. b) Fluorescence image of single molecules of **36** embedded in a polymer matrix. C) Imaging of lipid membranes of compartments in living HeLa cells after application of **36**. d) Structural formula of **37**.

A special feature of rylene dyes is that different functional groups can be placed independently within the imide structure or into the *bay* region.[33,39] In addition, the imide

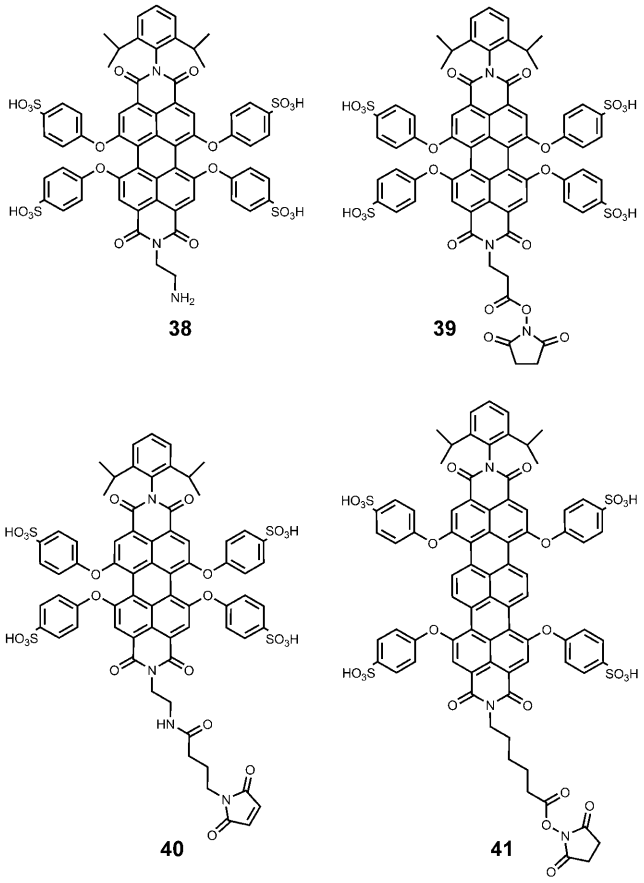

Figure 20. Overview of different PDI and TDI biolabels.

structure allows the introduction of two different kinds of substituents and, therefore, a single reactive group for biolabeling could be attached at this position.[179,180] In this way, water-soluble PDI and TDI dyes with four sulfonic acid groups as well as a single group that allows bioconjugation, for example, carboxylic acid or amino groups, suitable for formation of an amide bond with lysine, glutamic acid, or aspartic acid groups were obtained.[180] Chromophores **38**–**40** are highly soluble in water and have high fluorescence quantum yield. The higher homologue WS-TDI **41** absorbs above 600 nm and thus is well-suited for single-molecule and live-cell experiments. For example, a bioconjugate of WS-TDI **41** and DNA showed good resistance against photodegradation and photoblinking.[19] One of the most frequently used approaches for the selective labeling of proteins is based on the introduction of a cysteine point mutation at a desired location of a recombinant protein surface, while the chromophore possesses a group that reacts with thiols. PDI **40** with a maleimide group (Figure 20) represents an attractive fluorescent probe for targeting accessible thiol groups.[180] One of the most common techniques in molecular biology is the expression of proteins with an oligohistidine tail, which usually facilitates the isolation and purification of the protein on tailored columns containing nitrilotriacetic acid groups (NTA). This tag could also be addressed by chromophores carrying such a specific moiety. The attachment of an NTA group within the imide structure of PDI (PDI-NTA **42**; Figure 21) allows the site-specific labeling of proteins with an oligohistidine tag in the presence of nickel ions.[179]

In contrast to other previously reported NTA-functionalized chromophores, the photophysical properties of the PDI-NTA remained unchanged upon complexation with nickel

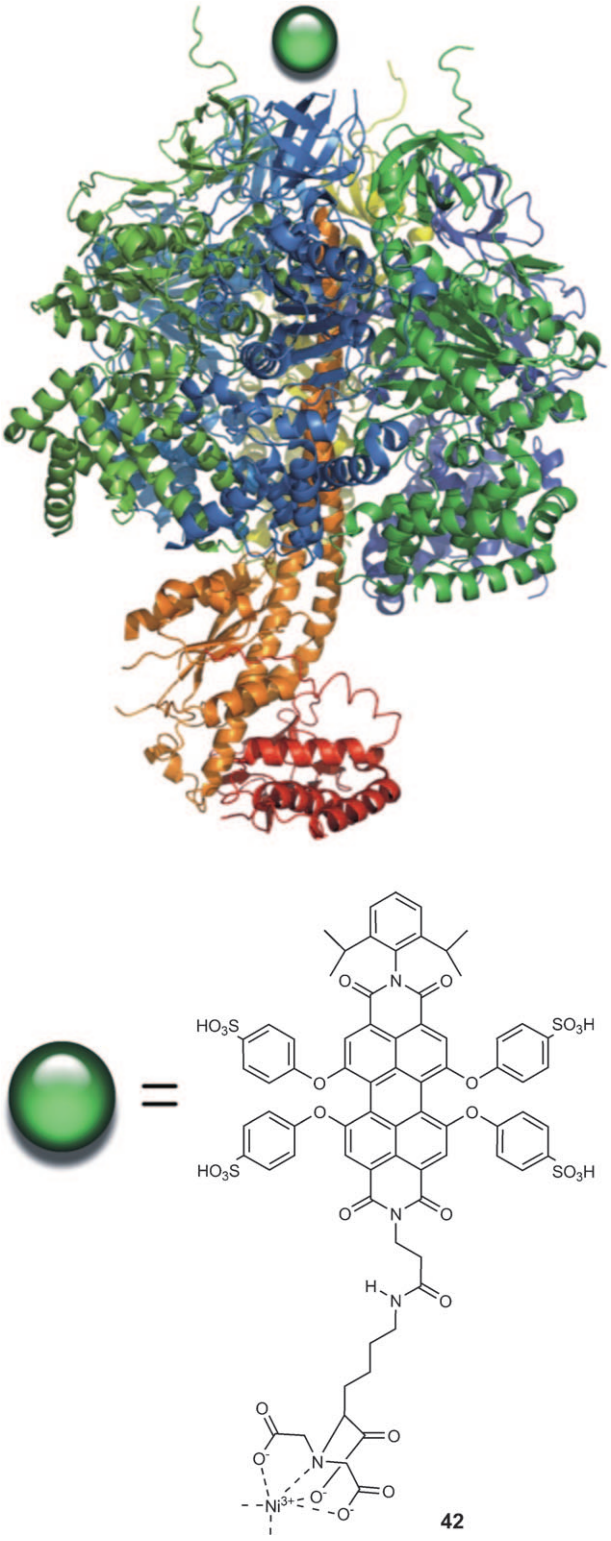

Figure 21. Protein labeling with the Ni-NTA-functionalized PDI dye **42** was successfully demonstrated using ATP synthase with an oligohistidine sequence.

ions.[181–183] Protein labeling with this NTA-functionalized perylene(dicarboximide) was successfully demonstrated by applying oligo-His-tagged ATP synthase.[179] In this context, it has been demonstrated that PDI-NTA is characterized by a stable emission wavelength and high emission intensity upon complexation with nickel ions. Such chromophores are particularly valuable for investigations of protein dynamics at the single-molecule level since the fluorescent reporter has a relatively small molecular weight (1555 $g\,mol^{-1}$), thus avoiding limitations arising from the large size of autofluorescent proteins or quantum dots. Therefore, the PDI-NTA chromophore offers great potential for the characterization of protein functions, dynamics, as well as their interaction partners.

6.3. Single Protein Spectroscopy

Single proteins, virions, drugs, and other single bioparticles have been labeled and their pathway and interactions have been followed inside living cells to elucidate their mechanism of cell uptake, trafficking, and interaction partners.[184] By using the asymmetric PDI chromophore **39**, single phospholipase enzymes were functionalized and visualized, even on a fluorescently labeled substrate.[180,185] Under these demanding conditions, the PDI **39** revealed survival times 600 times longer than with ATTO 647N,[177] which is often considered an ultrastable fluorescent reporter.[186] The enzymes labeled with this PDI dye allowed the actions of phospholipase on their natural substrates to be characterized, for example, on phospholipid-supported layers.[185] This approach enabled phospholipase mobilities to be correlated with the catalytic activities for the first time.[185] Furthermore, this assay allowed the validation of the influence of the layer composition and fluidity on both the phospholipase mobility and activity (Figure 22).[185]

We have shown in previous sections that the combination of the hydrophobic rylene scaffold and polar substituents can lead to the formation of highly amphiphilic molecules. These can serve as nanoreporters of the polarity of their direct surroundings, thus allowing the visualization of membranes with high contrast. This remarkable contrast is not only a result of the preference of such nanoemitters for lipophilic environments, but also supported by the formation of nonfluorescent chromophore aggregates in aqueous solution. In Section 6.4 we present the concept of achieving high subcellular specificities by the presence of multiple charges. Such water-soluble and fluorescent rylene polyelectrolytes display outstanding subcellular specificities for natural polyelectrolytes.

6.4. PDI-Polyelectrolytes with High Subcellular Specificity

Charges play an important role in cell biology. Negatively charged membranes regulate the cellular uptake and efflux of molecules or macromolecules.[187,188] In the cell nucleus, positively charged histone proteins form highly ordered histone octamers that interact tightly with negatively charged

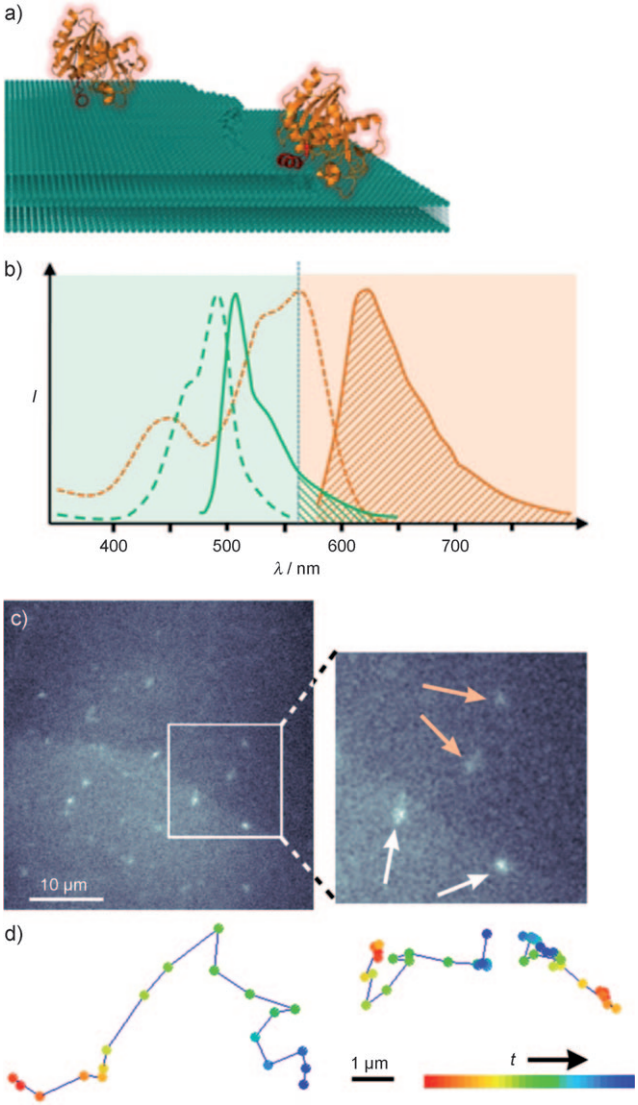

Figure 22. Single-protein spectroscopy of PDI **39** labeled phospholipase on the phospholipid substrate palmitoyl oleoyl phosphatidyl choline (POPC). a) Schematic representation demonstrating the concept of the experiment (phospholipid layers in green, individual phopholipases in yellow). b) Absorption (dashed lines) and emission spectra (full lines) of 3,3'-dioctadecyloxacarbocyanine perchlorate (DiO, used to stain the substrate layers) and PDI label **39** (used to stain the individual enzymes) in green and yellow, respectively. By selecting the right filter the PDI label **39** allows sufficient photons to be obtained to discriminate individual enzymes even with a fluorescence background from the layers. c) Labeling of the layers allows visualization of steps in the layers and in combination with the labeled enzymes also for visualization of preferential adsorption of enzyme molecules at the steps. The image was obtained after accumulating eight frames (400 ms) The white square corresponds to the magnified image on the right side where two enzymes are situated at the step between two POPC layers (white arrows) and two enzymes moving on a POPC layer (orange arrows). d) Trajectories of individual enzymes as a function of time. The left trajectory corresponds to an enzyme moving on a POCP layer, while the right trajectories correspond to enzymes situated at the edge between two layers. From such trajectories, the MDS of individual enzymes can be calculated. From these data diffusion constants can be extracted for single active enzymes operating at the edge of a layer, which vary between 0.07 and $1.7\times10^{-8}\ cm^2\,s^{-1}$.

DNA, thus forming the nucleosome for storing the genetic material.[189] The design of nanoemitters with a large number of positive or negative charges should enable electrostatic interactions with natural polyelectrolytes such as DNA or nuclear proteins. To date, little is known about the fate of polyelectrolytes in cells. This lack of information is mainly due to the fact that it is difficult to combine nanometer sizes, fluorescence, and multiple charges in one molecule. Our design concept is based on the fact that the attachment of dendritic branches to a central rylene core offers the introduction of a high number of substituents exclusively located at the periphery. This concept has been applied to the design of complex core–shell macromolecules consisting of a central PDI chromophore, surrounded by a hydrophobic polyphenylene shell. This core–shell structure offers access to molecular dimensions and protects the inner chromophore, as the outer shell bears multiple amino or carboxylic acid groups (Figure 23).[190–193] These macromolecules were synthesized by atom-transfer radical polymerization (ATRP) grafting from a fluorescent, polyphenylene macroinitiator. The number of charges was adjusted during the polymerization reaction.[190–193] The chain lengths were varied from 10 to 50 monomer units, and in this way the numbers of carboxylic acid and amino groups could be varied. In this way, macromolecules with 80–1280 polar surface groups were prepared.[193] Such PDI polyelectrolytes display high water solubility and moderate to good fluorescence quantum yields.[193] Interestingly, PDI nanoemitters with a high number of positive charges, for example, **44** (Figure 23b), showed fast cell uptake[192] and specific interaction with the highly negatively charged components of the extracellular matrix (ECM; Figure 23d).[194] The ECM surrounds cells and plays an important role in many aspects of cellular fate, including cell migration, stem cell differentiation, and cancer progression. The dendritic polyelectrolyte **44** with about 50 repeat units ($n = 50$) represents the first chromophore able to stain the ECM in both fixed and living preparations by strongly binding to its negatively charged constituents.[194] Even more remarkable, negatively charged PDI core–shell macromolecules bearing multiple carboxylic acid groups **43** were employed successfully to selectively stain the cell nucleus through specific interaction with positively charged nuclear proteins (histones; Figure 23c).

The formation of the complex was exemplarily studied by isothermal titration calorimetry after application of **43** to cationic lysine-rich histone proteins H1.[193] Very low dissociation constants in the low nanomolar range were calculated, which points towards tight interactions between **43** and H1. Interestingly, the emission intensities of the central PDI dye increased significantly after binding to the ECM or histone proteins, thus making these nanoemitters attractive for multiple channel fluorescence imaging studies.

7. Conclusions

We have shown in this Review that tailored rylene-based nanoemitters are prepared by the introduction of functional groups at distinct positions of the chromophore core. Their

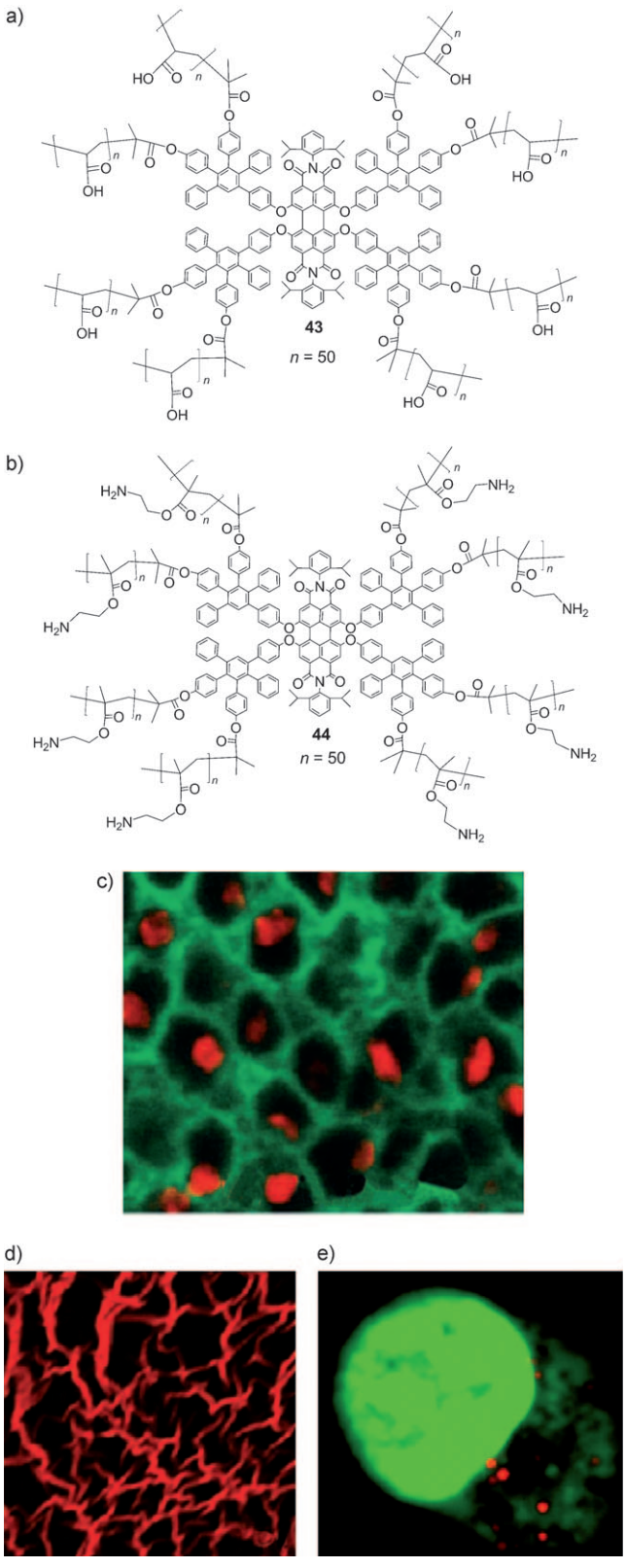

Figure 23. a) First-generation core–shell macromolecule **43** containing approximately 400 carboxylic acid groups within the outer shell. b) First-generation core–shell macromolecule **44** with about 400 primary amino groups. c) Confocal microscopy images of *Drosophila* larval tissue stained with **43**, which demonstrates exclusively nuclear localization. d) Confocal images of ECM staining with **44** in fixed wing epithelium. e) Uptake of **44** after 15 min into ECV-304 cells.

optical properties, solubility, as well as intra- and intermolecular interactions can be manipulated by the nature of the attached functional groups. In addition, the opportunity to decorate rylene chromophores with two different groups within the imide structure as well with various numbers of substituents within the *bay* region offers access to nonsymmetric chromophores that are attractive for the build-up of complex nanoscopic architectures, as nanoreporters, or as fluorescent markers for specific protein-staining experiments.

In this way, high-performance nanoemitters have been obtained that cover the whole visible light and near-infrared region of the spectrum, with distinct absorption and emission envelopes, high fluorescence quantum yields, and superior photostabilities. In particular, the positioning of polar or charged groups either on their scaffolds or within their direct surroundings has a significant impact on their optical properties. It has been shown that the high photostabilities of such nanoemitters means that they have great potential as single reporters of their local environment. Tailor-made rylene derivatives have enabled the study of polymer dynamics, polymerization kinetics, pore stuructures in mesoporous materials, and membrane uptake.

The concept of introducing rylene dyes as nanoreporters within a relative small volume has been brought to perfection in the case of dendritic multichromophores. The combination of more than one rylene chromophore at a distinct position within a defined nanoscopic volume offers the unique opportunity to study the results of varying the chromophore distances, orientations, and spectral overlap on energy- or electron-transfer processes at the single-molecule level. Such complex macromolecules allow a better understanding of phenomena such as the collective behavior of multichromophores, and pave the way towards improved synthetic light-harvesting arrays. The combination of nanoscopic rylene dyes with high numbers of positive or negative charges leads to the formation of core–shell polyelectrolytes that display outstanding subcellular specificities for natural polyelectrolytes such as DNA or histones.

The versatile and tunable properties of rylene dyes ensure that they will remain a cornerstone in the future development of high-performance functional dyes.

8. Abbreviations

5DI	pentarylenebis(dicarboximide)
ATRP	atom-transfer radical polymerization
Bodipy	4,4′-difluoro-4-bora-3a,4a-diaza-*s*-indacenes
CSS	charge-separated state
CTAB	cetyltrimethylammoniumbromide
DiO	3,3'-dioctadecyloxacarbocyanine
DSSC	dye-sensitized solar cells
ECM	extracellular matrix
ET	electron transfer
FCS	fluorescence correlation spectroscopy
FLIM	fluorescence lifetime imaging
FRET	Förster resonance energy transfer
GS	ground state
HDI	hexarylenebis(dicarboximide)
HOMO	highest occupied molecular orbital
HT	hole transport
ISC	intersystem crossing
ITO	indium tin oxide
LES	locally excited state
LH2	light-harvesting antenna complex
LUMO	lowest occupied molecular orbital
MSD	mean-square deviation
NIR	near infrared
NMI	naphthalenemonoimide
NTA	nitrilotriacetic acid
PDI	perylenebis(dicarboximide)
PEO	polyethyleneoxide
PMI	perylene-3,4-dicarboximide
PMMA	polymethylmethacrylate
PnBMA	poly(*n*-butylmethacrylate)
POPC	1-palmitoyl-2-oleoyl-*sn*-glycero-3-phosphocholine
QDI	quaterrylenebis(dicarboximide)
SAM	self-assembled monolayer
SMS	single-molecule spectroscopy
STED	stimulated emission depletion
T_g	glass-transition temperature
TDI	terrylenebis(dicarboximide)
TPA	triphenylamine
WFM	wide-field microscopy
WS-TDI	1,6,7,12-tetra(4-sulfonylphenoxy)-*N*,*N*-(2,6-diisopropylphenyl)terrylene-3,4:9,10-tetracarboxidiimide

We would like to thank all the people who performed the work presented herein. EU financial support through the Integrated Project NAIMO (no. NMP4-CT-2004-500355) is gratefully acknowledged. This work, as part of the European Science Foundation EUROCORES Programme SONS, was supported by funds from the FWO (Fonds voor wetenschappelijk onderzoek Vlaanderen), the DFG (Deutsche Forschungsgemeinschaft), and the EC 6th Framework Program (ERAS-CT-2003-980409). We also acknowledge financial support from the Sonderforschungsbereich SFB 625 and the DFG within the frame of the "Elementarprozesse der organischen Photovoltaik" Mu 334/31-1. T.V. would like to thank the FWO and the UNIK – Synthetic Biology program (grant 09-065274) for financial support. We would like to thank Ashlan Musante, Andrew Yeung, and Chen Li for their help when preparing the manuscript.

Received: May 13, 2009
Revised: January 22, 2010
Published online: October 25, 2010

[1] K. V. Datye, *Colourage Annu.* **1988**, *3*, 0.
[2] J. Lee, *Textile Wet Processing: Preparation, Dyeing and Finishing of Today's Textile Fabrics* [Conference] **1998**, VIII/0.
[3] V. G. Agnihotri, *Colourage* **1976**, *23*, 1.
[4] H. Zollinger, *Color Chemistry*, 3rd ed., Wiley-VCH, New York, **2001**.

[5] Z. Chen, A. Lohr, C. R. Saha-Möller, F. Würthner, *Chem. Soc. Rev.* **2009**, *38*, 564.
[6] G. Ulrich, R. Ziessel, A. Harriman, *Angew. Chem.* **2008**, *120*, 1202; *Angew. Chem. Int. Ed.* **2008**, *47*, 1184.
[7] N. S. Finney, *Curr. Opin. Chem. Biol.* **2006**, *10*, 238.
[8] U. Resch-Genger, M. Grabolle, S. Cavaliere-Jaricot, R. Nitschke, T. Nann, *Nat. Methods* **2008**, *5*, 763.
[9] S. M. Melnikov, E. K. L. Yeow, H. Uji-i, M. Cotlet, K. Müllen, F. C. De Schryver, J. Enderlein, J. Hofkens, *J. Phys. Chem. B* **2007**, *111*, 708.
[10] C. Jung, B. K. Müller, D. C. Lamb, F. Nolde, K. Müllen, C. Bräuchle, *J. Am. Chem. Soc.* **2006**, *128*, 5283.
[11] F. Würthner, *Chem. Commun.* **2004**, 1564.
[12] J. Kirstein, B. Platschek, C. Jung, R. Brown, T. Bein, C. Bräuchle, *Nat. Mater.* **2007**, *6*, 303.
[13] R. Métivier, F. Nolde, K. Müllen, T. Basché, *Phys. Rev. Lett.* **2007**, *98*, 047802.
[14] E. Clar, *Chem. Ber.* **1948**, *81*, 52.
[15] L. Zang, Y. Che, J. S. Moore, *Acc. Chem. Res.* **2008**, *41*, 1596.
[16] X. Meng, W. Zhu, H. Tian, *Opt. Sci. Eng.* **2008**, *133*, 129.
[17] R. Schroeder, B. Ullrich, *OSA Trends Opt. Photonics Ser.* **2002**, *64*, 115.
[18] A. C. Grimsdale, K. Müllen, *Angew. Chem.* **2005**, *117*, 5732; *Angew. Chem. Int. Ed.* **2005**, *44*, 5592.
[19] C. Jung, N. Ruthardt, R. Lewis, J. Michaelis, B. Sodeik, F. Nolde, K. Peneva, K. Müllen, C. Bräuchle, *ChemPhysChem* **2009**, *10*, 180.
[20] A. Liscio, G. De Luca, F. Nolde, V. Palermo, K. Müllen, P. Samori, *J. Am. Chem. Soc.* **2008**, *130*, 780.
[21] J. P. Schmidtke, R. H. Friend, M. Kastler, K. Müllen, *J. Chem. Phys.* **2006**, *124*, 174704.
[22] K. Bouchemal, *Drug Discovery Today* **2008**, *13*, 960.
[23] M. A. Angadi, D. Gosztola, M. R. Wasielewski, *J. Appl. Phys.* **1998**, *83*, 6187.
[24] Z. Chen, M. G. Debije, T. Debaerdemaeker, P. Osswald, F. Würthner, *ChemPhysChem* **2004**, *5*, 137.
[25] R. Gomez, J. L. Segura, *Handb. Org. Electron. Photonics* **2008**, *3*, 351.
[26] S. Becker, A. Bohm, K. Müllen, *Chem. Eur. J.* **2000**, *6*, 3984.
[27] F. D. Stefani, C. Kohl, Y. S. Avlasevich, N. Horn, A. K. Vogt, K. Müllen, M. Kreiter, *Chem. Mater.* **2006**, *18*, 6115.
[28] P. Tinnefeld, K. D. Weston, T. Vosch, M. Cotlet, T. Weil, J. Hofkens, K. Müllen, F. C. De Schryver, M. Sauer, *J. Am. Chem. Soc.* **2002**, *124*, 14310.
[29] S. Tasch, E. J. W. List, O. Ekstrom, W. Graupner, G. Leising, P. Schlichting, U. Rohr, Y. Geerts, U. Scherf, K. Müllen, *Appl. Phys. Lett.* **1997**, *71*, 2883.
[30] S. Tasch, E. J. W. List, C. Hochfilzer, G. Leising, P. Schlichting, U. Rohr, Y. Geerts, U. Scherf, K. Müllen, *Phys. Rev. B* **1997**, *56*, 4479.
[31] P. Posch, M. Thelakkat, H. W. Schmidt, *Synth. Met.* **1999**, *102*, 1110.
[32] S. Schols, S. Verlaak, C. Rolin, D. Cheyns, J. Genoe, P. Heremans, *Adv. Funct. Mater.* **2008**, *18*, 136.
[33] N. G. Pschirer, C. Kohl, F. Nolde, J. Qu, K. Müllen, *Angew. Chem.* **2006**, *118*, 1429; *Angew. Chem. Int. Ed.* **2006**, *45*, 1401.
[34] F. Kulzer, M. Orrit, *Annu. Rev. Phys. Chem.* **2004**, *55*, 585.
[35] H. Langhals, *Helv. Chim. Acta* **2005**, *88*, 1309.
[36] F. Nolde, J. Qu, C. Kohl, N. G. Pschirer, E. Reuther, K. Müllen, *Chem. Eur. J.* **2005**, *11*, 3959.
[37] H. Quante, K. Müllen, *Angew. Chem.* **1995**, *107*, 1487; *Angew. Chem. Int. Ed.* **1995**, *34*, 1323.
[38] Y. Geerts, H. Quante, H. Platz, R. Mahrt, M. Hopmeier, A. Bohm, K. Müllen, *J. Mater. Chem.* **1998**, *8*, 2357.
[39] A. Herrmann, K. Müllen, *Chem. Lett.* **2006**, *35*, 978.
[40] Y. Avlasevich, S. Mueller, P. Erk, K. Müllen, *Chem. Eur. J.* **2007**, *13*, 6555.
[41] S. Müller, K. Müllen, *Chem. Commun.* **2005**, 4045.
[42] C. Kohl, T. Weil, J. Qu, K. Müllen, *Chem. Eur. J.* **2004**, *10*, 5297.
[43] A. Herrmann, T. Weil, V. Sinigersky, U. M. Wiesler, T. Vosch, J. Hofkens, F. C. De Schryver, K. Müllen, *Chem. Eur. J.* **2001**, *7*, 4844.
[44] D. Wöll, H. Uji-I, T. Schnitzler, J. I. Hotta, P. Dedecker, A. Herrmann, F. C. De Schryver, K. Müllen, J. Hofkens, *Angew. Chem.* **2008**, *120*, 795; *Angew. Chem. Int. Ed.* **2008**, *47*, 783.
[45] R. Yasukuni, T. Asahi, T. Sugiyama, H. Masuhara, M. Sliwa, J. Hofkens, F. C. De Schryver, M. Van der Auweraer, A. Herrmann, K. Muller, *Appl. Phys. A* **2008**, *93*, 5.
[46] R. Yasukuni, M. Sliwa, J. Hofkens, F. C. De Schryver, A. Herrmann, K. Müllen, T. Asahi, H. Masuhara, *Jpn. J. Appl. Phys.* **2009**, *93*, 5.
[47] E. Fron, R. Pilot, G. Schweitzer, J. Q. Qu, A. Herrmann, K. Müllen, J. Hofkens, M. van der Auweraer, F. C. De Schryver, *Photochem. Photobiol. Sci.* **2008**, *7*, 597.
[48] J. Hofkens, T. Vosch, M. Maus, F. Kohn, M. Cotlet, T. Weil, A. Herrmann, K. Müllen, F. C. De Schryver, *Chem. Phys. Lett.* **2001**, *333*, 255.
[49] E. Fron, G. Schweitzer, P. Osswald, F. Würthner, P. Marsal, D. Beljonne, K. Müllen, F. C. De Schryver, M. Van der Auweraer, *Photochem. Photobiol. Sci.* **2008**, *7*, 1509.
[50] P. Osswald, F. Würthner, *J. Am. Chem. Soc.* **2007**, *129*, 14319.
[51] M. Cotlet, T. Vosch, S. Habuchi, T. Weil, K. Müllen, J. Hofkens, F. De Schryver, *J. Am. Chem. Soc.* **2005**, *127*, 9760.
[52] H. Uji-i, S. M. Melnikov, A. Deres, G. Bergamini, F. De Schryver, A. Herrmann, K. Müllen, J. Enderlein, J. Hofkens, *Polymer* **2006**, *47*, 2511.
[53] C. Li, J. Schoeneboom, Z. Liu, N. G. Pschirer, P. Erk, A. Herrmann, K. Müllen, *Chem. Eur. J.* **2009**, *15*, 878.
[54] W. E. Moerner, M. Orrit, *Science* **1999**, *283*, 1670.
[55] S. M. Nie, D. T. Chiu, R. N. Zare, *Science* **1994**, *266*, 1018.
[56] D. A. VandenBout, W. T. Yip, D. H. Hu, D. K. Fu, T. M. Swager, P. F. Barbara, *Science* **1997**, *277*, 1074.
[57] P. Tinnefeld, M. Sauer, *Angew. Chem.* **2005**, *117*, 2698; *Angew. Chem. Int. Ed.* **2005**, *44*, 2642.
[58] F. C. De Schryver, T. Vosch, M. Cotlet, M. Van der Auweraer, K. Müllen, J. Hofkens, *Acc. Chem. Res.* **2005**, *38*, 514.
[59] C. Eggeling, J. Widengren, R. Rigler, C. A. M. Seidel, *Anal. Chem.* **1998**, *70*, 2651.
[60] T. Basché, S. Kummer, C. Bräuchle, *Nature* **1995**, *373*, 132.
[61] D. Wöll, E. Braeken, A. Deres, F. C. De Schryver, H. Uji-i, J. Hofkens, *Chem. Soc. Rev.* **2009**, *38*, 313.
[62] X. Michalet, S. Weiss, *C. R. Phys.* **2002**, *3*, 619.
[63] M. Orrit, *J. Chem. Phys.* **2002**, *117*, 10938.
[64] P. F. Barbara, *Acc. Chem. Res.* **2005**, *38*, 503.
[65] D.-P. Herten, *Chem. Unserer Zeit* **2008**, *42*, 192.
[66] P. Schlichting, B. Duchscherer, G. Seisenberger, T. Basche, C. Bräuchle, K. Müllen, *Chem. Eur. J.* **1999**, *5*, 2388.
[67] M. W. Holman, R. C. Liu, L. Zang, P. Yan, S. A. DiBenedetto, R. D. Bowers, D. M. Adams, *J. Am. Chem. Soc.* **2004**, *126*, 16126.
[68] J. Hernando, P. A. J. de Witte, E. van Dijk, J. Korterik, R. J. M. Nolte, A. E. Rowan, M. F. Garcia-Parajo, N. F. van Hulst, *Angew. Chem.* **2004**, *116*, 4137; *Angew. Chem. Int. Ed.* **2004**, *43*, 4045.
[69] J. P. Hoogenboom, J. Hernando, E. van Dijk, N. F. van Hulst, M. F. Garcia-Parajo, *ChemPhysChem* **2007**, *8*, 823.
[70] J. N. Clifford, T. D. M. Bell, P. Tinnefeld, M. Heilemann, S. M. Melnikov, J. Hotta, M. Sliwa, P. Dedecker, M. Sauer, J. Hofkens, E. K. L. Yeow, *J. Phys. Chem. B* **2007**, *111*, 6987.
[71] E. K. L. Yeow, S. M. Melnikov, T. D. M. Bell, F. C. De Schryver, J. Hofkens, *J. Phys. Chem. A* **2006**, *110*, 1726.
[72] F. Cichos, C. von Borczyskowski, M. Orrit, *Curr. Opin. Colloid Interface Sci.* **2007**, *12*, 272.

[73] F. Köhn, J. Hofkens, R. Gronheid, M. Van der Auweraer, F. C. De Schryver, *J. Phys. Chem. A* **2002**, *106*, 4808.
[74] W. T. Yip, D. H. Hu, J. Yu, D. A. Vanden Bout, P. F. Barbara, *J. Phys. Chem. A* **1998**, *102*, 7564.
[75] K. D. Weston, P. J. Carson, H. Metiu, S. K. Buratto, *J. Chem. Phys.* **1998**, *109*, 7474.
[76] E. Betzig, G. H. Patterson, R. Sougrat, O. W. Lindwasser, S. Olenych, J. S. Bonifacino, M. W. Davidson, J. Lippincott-Schwartz, H. F. Hess, *Science* **2006**, *313*, 1642.
[77] S. Bretschneider, C. Eggeling, S. W. Hell, *Phys. Rev. Lett.* **2007**, *98*, 218103.
[78] C. Flors, J. Hotta, H. Uji-I, P. Dedecker, R. Ando, H. Mizuno, A. Miyawaki, J. Hofkens, *J. Am. Chem. Soc.* **2007**, *129*, 13970.
[79] J. Fölling, V. Belov, R. Kunetsky, R. Medda, A. Schönle, A. Egner, C. Eggeling, M. Bossi, S. W. Hell, *Angew. Chem.* **2007**, *119*, 6382; *Angew. Chem. Int. Ed.* **2007**, *46*, 6266.
[80] J. Fölling, M. Bossi, H. Bock, R. Medda, C. A. Wurm, B. Hein, S. Jakobs, C. Eggeling, S. W. Hell, *Nat. Methods* **2008**, *5*, 943.
[81] M. Heilemann, E. Margeat, R. Kasper, M. Sauer, P. Tinnefeld, *J. Am. Chem. Soc.* **2005**, *127*, 3801.
[82] M. Heilemann, S. van de Linde, M. Schüttpelz, R. Kasper, B. Seefeldt, A. Mukherjee, P. Tinnefeld, M. Sauer, *Angew. Chem.* **2008**, *120*, 6266; *Angew. Chem. Int. Ed.* **2008**, *47*, 6172.
[83] S. W. Hell, *Science* **2007**, *316*, 1153.
[84] S. T. Hess, T. P. K. Girirajan, M. D. Mason, *Biophys. J.* **2006**, *91*, 4258.
[85] S. v. d. Linde, U. Endesfelder, A. Mukherjee, M. Schüttpelz, G. Wiebusch, S. Wolter, M. Heilemann, M. Sauer, *Photochem. Photobiol. Sci.* **2009**, *8*, 465.
[86] M. J. Rust, M. Bates, X. W. Zhuang, *Nat. Methods* **2006**, *3*, 793.
[87] S. van de Linde, M. Sauer, M. Heilemann, *J. Struct. Biol.* **2008**, *164*, 250.
[88] J. Vogelsang, T. Cordes, P. Tinnefeld, *Photochem. Photobiol. Sci.* **2009**, 8, 486.
[89] P. G. Debenedetti, F. H. Stillinger, *Nature* **2001**, *410*, 259.
[90] A. P. Bartko, R. M. Dickson, *J. Phys. Chem. B* **1999**, *103*, 11237.
[91] A. P. Bartko, R. M. Dickson, *J. Phys. Chem. B* **1999**, *103*, 3053.
[92] R. M. Dickson, D. J. Norris, W. E. Moerner, *Phys. Rev. Lett.* **1998**, *81*, 5322.
[93] A. P. Bartko, K. W. Xu, R. M. Dickson, *Phys. Rev. Lett.* **2002**, *89*, 026101.
[94] L. A. Deschenes, D. A. Vanden Bout, *J. Chem. Phys.* **2002**, *116*, 5850.
[95] C. Y. J. Wei, Y. H. Kim, R. K. Darst, P. J. Rossky, D. A. Vanden Bout, *Phys. Rev. Lett.* **2005**, *95*, 173001.
[96] P. Dedecker, B. Muls, A. Deres, H. Uji-i, J. Hotta, M. Sliwa, J. P. Soumillion, K. Müllen, J. Enderlein, J. Hofkens, *Adv. Mater.* **2009**, *21*, 1079.
[97] C. Jung, J. Kirstein, B. Platschek, T. Bein, M. Budde, I. Frank, K. Müllen, J. Michaelis, C. Bräuchle, *J. Am. Chem. Soc.* **2008**, *130*, 1638.
[98] A. Zürner, J. Kirstein, M. Döblinger, C. Bräuchle, T. Bein, *Nature* **2007**, *450*, 705.
[99] S. W. Hell, J. Wichmann, *Optics Letters* **1994**, *19*, 780.
[100] B. Harke, J. Keller, C. K. Ullal, V. Westphal, A. Schoenle, S. W. Hell, *Optics Express* **2008**, *16*, 4154.
[101] T. A. Klar, S. Jakobs, M. Dyba, A. Egner, S. W. Hell, *Proc. Natl. Acad. Sci. USA* **2000**, *97*, 8206.
[102] O. Siiman, A. Jitianu, M. Bele, P. Grom, E. Matijevic, *J. Colloid Interface Sci.* **2007**, *309*, 8.
[103] M. B. J. Roeffaers, G. De Cremer, H. Uji-i, B. Muls, B. F. Sels, P. A. Jacobs, F. C. De Schryver, D. E. De Vos, J. Hofkens, *Proc. Natl. Acad. Sci. USA* **2007**, *104*, 12603.
[104] M. B. J. Roeffaers, B. F. Sels, H. Uji-i, F. C. De Schryver, P. A. Jacobs, D. E. De Vos, J. Hofkens, *Nature* **2006**, *439*, 572.
[105] R. Ameloot, M. Roeffaers, M. Baruah, G. De Cremer, B. Sels, D. De Vos, J. Hofkens, *Photochem. Photobiol. Sci.* **2009**, *8*, 453.
[106] S. Jansson, *Encycl. Biol. Chem.* **2004**, *2*, 567.
[107] P. Horton, A. V. Ruban, R. G. Walters, *Annu. Rev. Pl. Phys. Pl. Mol. Biol.* **1996**, *47*, 655.
[108] R. MacColl, *J. Struct. Biol.* **1998**, *124*, 311.
[109] R. Y. Tsien, *Annu. Rev. Biochem.* **1998**, *67*, 509.
[110] S. Berciaud, L. Cognet, G. A. Blab, B. Lounis, *Phys. Rev. Lett.* **2004**, *93*, 257402.
[111] S. Berciaud, L. Cognet, B. Lounis, *Nano Lett.* **2005**, *5*, 2160.
[112] S. Berciaud, L. Cognet, P. Tamarat, B. Lounis, *Nano Lett.* **2005**, *5*, 515.
[113] B. Lounis, M. Orrit, *Rep. Prog. Phys.* **2005**, *68*, 1129.
[114] M. Treguer, F. Rocco, G. Lelong, A. Le Nestour, T. Cardinal, A. Maali, B. Lounis, *Solid State Sci.* **2005**, *7*, 812.
[115] F. Vögtle, N. Werner, G. Richardt, *Dendritische Moleküle: Konzepte, Synthesen, Eigenschaften, Anwendungen*, *1st ed.*, Vieweg + Teubner, Wiesbaden, **2007**.
[116] R. E. Bauer, C. G. Clark, Jr., M. Klapper, L. Zhi, K. Müllen, *Polym. Prepr. Am. Chem. Soc. Div. Polym. Chem.* **2007**, *48*, 49.
[117] H. Zhang, P. C. M. Grim, P. Foubert, T. Vosch, P. Vanoppen, U. M. Wiesler, A. J. Berresheim, K. Müllen, F. C. De Schryver, *Langmuir* **2000**, *16*, 9009.
[118] A. C. Grimsdale, T. Vosch, M. Lor, M. Cotlet, S. Habuchi, J. Hofkens, F. C. De Schryver, K. Müllen, *J. Lumin.* **2005**, *111*, 239.
[119] D. J. Liu, S. De Feyter, M. Cotlet, A. Stefan, U. M. Wiesler, A. Herrmann, D. Grebel-Koehler, J. Q. Qu, K. Müllen, F. C. De Schryver, *Macromolecules* **2003**, *36*, 5918.
[120] H. Wolf-Klein, C. Kohl, K. Müllen, H. Paulsen, *Angew. Chem.* **2002**, *114*, 3526; *Angew. Chem. Int. Ed.* **2002**, *41*, 3378.
[121] T. Gensch, J. Hofkens, A. Heirmann, K. Tsuda, W. Verheijen, T. Vosch, T. Christ, T. Basche, K. Müllen, F. C. De Schryver, *Angew. Chem.* **1999**, *111*, 3970; *Angew. Chem. Int. Ed.* **1999**, *38*, 3752.
[122] J. Hofkens, L. Latterini, G. De Belder, T. Gensch, M. Maus, T. Vosch, Y. Karni, G. Schweitzer, F. C. De Schryver, A. Hermann, K. Müllen, *Chem. Phys. Lett.* **1999**, *304*, 1.
[123] J. Hofkens, M. Maus, T. Gensch, T. Vosch, M. Cotlet, F. Kohn, A. Herrmann, K. Müllen, F. De Schryver, *J. Am. Chem. Soc.* **2000**, *122*, 9278.
[124] M. Maus, R. De, M. Lor, T. Weil, S. Mitra, U. M. Wiesler, A. Herrmann, J. Hofkens, T. Vosch, K. Müllen, F. C. De Schryver, *J. Am. Chem. Soc.* **2001**, *123*, 7668.
[125] T. Vosch, J. Hofkens, M. Cotlet, F. Kohn, H. Fujiwara, R. Gronheid, K. Van Der Biest, T. Weil, A. Herrmann, K. Müllen, S. Mukamel, M. Van der Auweraer, F. C. De Schryver, *Angew. Chem.* **2001**, *113*, 4779; *Angew. Chem. Int. Ed.* **2001**, *40*, 4643.
[126] T. Vosch, M. Cotlet, J. Hofkens, K. Van der Biest, M. Lor, K. Weston, P. Tinnefeld, M. Sauer, L. Latterini, K. Müllen, F. C. De Schryver, *J. Phys. Chem. A* **2003**, *107*, 6920.
[127] S. Masuo, T. Vosch, M. Cotlet, P. Tinnefeld, S. Habuchi, T. D. M. Bell, I. Oesterling, D. Beljonne, B. Champagne, K. Müllen, M. Sauer, J. Hofkens, F. C. De Schryver, *J. Phys. Chem. B* **2004**, *108*, 16686.
[128] W. Schroeyers, R. Vallee, D. Patra, J. Hofkens, S. Habuchi, T. Vosch, M. Cotlet, K. Müllen, J. Enderlein, F. C. De Schryver, *J. Am. Chem. Soc.* **2004**, *126*, 14310.
[129] P. Tinnefeld, J. Hofkens, D. P. Herten, S. Masuo, T. Vosch, M. Cotlet, S. Habuchi, K. Müllen, F. C. De Schryver, M. Sauer, *ChemPhysChem* **2004**, *5*, 1786.
[130] T. Weil, U. M. Wiesler, A. Herrmann, R. Bauer, J. Hofkens, F. C. De Schryver, K. Müllen, *J. Am. Chem. Soc.* **2001**, *123*, 8101.
[131] I. Oesterling, K. Müllen, *J. Am. Chem. Soc.* **2007**, *129*, 4595.
[132] T. Förster, *Ann. Phys.* **1948**, *437*, 55.
[133] J. Hofkens, M. Cotlet, T. Vosch, P. Tinnefeld, K. D. Weston, C. Ego, A. Grimsdale, K. Müllen, D. Beljonne, J. L. Bredas, S.

Jordens, G. Schweitzer, M. Sauer, F. De Schryver, *Proc. Natl. Acad. Sci. USA* **2003**, *100*, 13146.
[134] M. Maus, S. Mitra, M. Lor, J. Hofkens, T. Weil, A. Herrmann, K. Müllen, F. C. De Schryver, *J. Phys. Chem. A* **2001**, *105*, 3961.
[135] G. De Belder, G. Schweitzer, S. Jordens, M. Lor, S. Mitra, J. Hofkens, S. De Feyter, M. Van der Auweraer, A. Herrmann, T. Weil, K. Müllen, F. C. De Schryver, *ChemPhysChem* **2001**, *2*, 49.
[136] M. Sliwa, C. Flors, I. Oesterling, J. Hotta, K. Müllen, F. C. De Schryver, J. Hofkens, *J. Phys. Condens. Matter* **2007**, *19*, 445004.
[137] C. Flors, I. Oesterling, T. Schnitzler, E. Fron, G. Schweitzer, M. Sliwa, A. Herrmann, M. van der Auweraer, F. C. de Schryver, K. Müllen, J. Hofkens, *J. Phys. Chem. C* **2007**, *111*, 4861.
[138] T. D. M. Bell, S. Habuchi, S. Masuo, I. Osterling, K. Müllen, P. Tinnefeld, M. Sauer, M. van der Auweraer, J. Hofkens, F. C. De Schryver, in Conference of the Physical Chemistry Division of the Royal-Australian-Chemistry-Institute, Hobart (Australia), **2004**, p. 1169.
[139] C. Hippius, I. H. M. van Stokkum, M. Gsanger, M. M. Groeneveld, R. M. Williams, F. Würthner, *J. Phys. Chem. C* **2008**, *112*, 2476.
[140] G. McDermott, S. M. Prince, A. A. Freer, A. M. Hawthornthwaite-Lawless, M. Z. Papiz, R. J. Cogdell, N. W. Isaacs, *Nature* **1995**, *374*, 517.
[141] G. D. Scholes, *Annu. Rev. Phys. Chem.* **2003**, *54*, 57.
[142] R. Jimenez, S. N. Dikshit, S. E. Bradforth, G. R. Fleming, *J. Phys. Chem.* **1996**, *100*, 6825.
[143] J. Yang, M. Park, Z. S. Yoon, T. Hori, X. B. Peng, N. Aratani, P. Dedecker, J. I. Hotta, H. Uji-I, M. Sliwa, J. Hofkens, A. Osuka, D. Kim, *J. Am. Chem. Soc.* **2008**, *130*, 1879.
[144] M. Park, M. C. Yoon, Z. S. Yoon, T. Hori, X. B. Peng, N. Aratani, J. I. Hotta, H. Uji-i, M. Sliwa, J. Hofkens, A. Osuka, D. Kim, *J. Am. Chem. Soc.* **2007**, *129*, 3539.
[145] K. Becker, P. G. Lagoudakis, G. Gaefke, S. Hoger, J. M. Lupton, *Angew. Chem.* **2007**, *119*, 3520; *Angew. Chem. Int. Ed.* **2007**, *46*, 3450.
[146] J. M. Serin, D. W. Brousmiche, J. M. J. Frechet, *Chem. Commun.* **2002**, 2605.
[147] M. Gingras, V. Placide, J. M. Raimundo, G. Bergamini, P. Ceroni, V. Balzani, *Chem. Eur. J.* **2008**, *14*, 10357.
[148] G. Hinze, R. Métivier, F. Nolde, K. Müllen, T. Basché, *J. Chem. Phys.* **2008**, *128*, 124516.
[149] G. Hinze, M. Haase, F. Nolde, K. Müllen, T. Basché, *J. Phys. Chem. A* **2005**, *109*, 6725.
[150] P. G. Van Patten, A. P. Shreve, J. S. Lindsay, R. J. Donohoe, *J. Phys. Chem. B* **1998**, *102*, 4209.
[151] M. Heilemann, P. Tinnefeld, G. S. Mosteiro, M. G. Parajo, N. F. Van Hulst, M. Sauer, *J. Am. Chem. Soc.* **2004**, *126*, 6514.
[152] M. Heilemann, R. Kasper, P. Tinnefeld, M. Sauer, *J. Am. Chem. Soc.* **2006**, *128*, 16864.
[153] A. Adronov, J. M. J. Frechet, *Chem. Commun.* **2000**, 1701.
[154] M. Maus, E. Rousseau, M. Cotlet, G. Schweitzer, J. Hofkens, M. Van der Auweraer, F. C. De Schryver, A. Krueger, *Rev. Sci. Instrum.* **2001**, *72*, 36.
[155] U. M. Wiesler, T. Weil, K. Müllen, *Top. Curr. Chem.* **2001**, *212*, 1.
[156] R. Gronheid, J. Hofkens, F. Kohn, T. Weil, E. Reuther, K. Müllen, F. C. De Schryver, *J. Am. Chem. Soc.* **2002**, *124*, 2418.
[157] M. Cotlet, R. Gronheid, S. Habuchi, A. Stefan, A. Barbafina, K. Müllen, J. Hofkens, F. C. De Schryver, *J. Am. Chem. Soc.* **2003**, *125*, 13609.
[158] T. Weil, E. Reuther, K. Müllen, *Angew. Chem.* **2002**, *114*, 1980; *Angew. Chem. Int. Ed.* **2002**, *41*, 1900.
[159] B. K. Kaletas, R. Dobrawa, A. Sautter, F. Würthner, M. Zimine, L. De Cola, R. M. Williams, *J. Phys. Chem. A* **2004**, *108*, 1900.
[160] M. J. Ahrens, L. E. Sinks, B. Rybtchinski, W. H. Liu, B. A. Jones, J. M. Giaimo, A. V. Gusev, A. J. Goshe, D. M. Tiede, M. R. Wasielewski, *J. Am. Chem. Soc.* **2004**, *126*, 8284.
[161] M. W. Holman, R. C. Liu, D. M. Adams, *J. Am. Chem. Soc.* **2003**, *125*, 12649.
[162] T. D. M. Bell, A. Stefan, S. Masuo, T. Vosch, M. Lor, M. Cotlet, J. Hofkens, S. Bernhardt, K. Müllen, M. van der Auweraer, J. W. Verhoeven, F. C. De Schryver, *ChemPhysChem* **2005**, *6*, 942.
[163] M. Cotlet, S. Masuo, M. Lor, E. Fron, M. Van der Auweraer, K. Müllen, J. Hofkens, F. De Schryver, *Angew. Chem.* **2004**, *116*, 6242; *Angew. Chem. Int. Ed.* **2004**, *43*, 6116.
[164] M. Cotlet, S. Masuo, G. Luo, J. Hofkens, M. van der Auweraer, J. Verhoeven, K. Müllen, X. S. Xie, F. de Schryver, *Proc. Natl. Acad. Sci. USA* **2004**, *101*, 14343.
[165] J. Qu, J. Zhang, A. C. Grimsdale, K. Müllen, F. Jaiser, X. Yang, D. Neher, *Macromolecules* **2004**, *37*, 8297.
[166] J. E. Moser, *Nat. Mater.* **2005**, *4*, 723.
[167] Y. Shirota, Y. Kuwabara, H. Inada, T. Wakimoto, H. Nakada, Y. Yonemoto, S. Kawami, K. Imai, *Appl. Phys. Lett.* **1994**, *65*, 807.
[168] S. Djurovic, N. Iversen, S. Jeansson, F. Hoover, G. Christensen, *Mol. Biotechnol.* **2004**, *28*, 21.
[169] T. Weil, M. A. Abdalla, C. Jatzke, J. Hengstler, K. Müllen, *Biomacromolecules* **2005**, *6*, 68.
[170] J. Rodríguez-Hernádez, J. Qu, E. Reuther, H.-A. Klok, K. Müllen, *Polym. Bull.* **2004**, *52*, 57.
[171] A. Margineanu, J. Hotta, R. A. Vallée, M. Van der Auweraer, M. Ameloot, A. Stefan, D. Beljonne, Y. Engelborghs, A. Herrmann, K. Müllen, F. C. De Schryver, J. Hofkens, *Biophys. J.* **2007**, *93*, 2877.
[172] R. A. L. Vallée, M. Cotlet, M. Van der Auweraer, J. Hofkens, K. Müllen, F. C. De Schryver, *J. Am. Chem. Soc.* **2004**, *126*, 2296.
[173] J. Qu, C. Kohl, M. Pottek, K. Müllen, *Angew. Chem.* **2004**, *116*, 1554; *Angew. Chem. Int. Ed.* **2004**, *43*, 1528.
[174] B. N. G. Giepmans, S. R. Adams, M. H. Ellisman, R. Y. Tsien, *Science* **2006**, *312*, 217.
[175] T. Ha, T. Enderle, D. F. Ogletree, D. S. Chemla, P. R. Selvin, S. Weiss, *Proc. Natl. Acad. Sci. USA* **1996**, *93*, 6264.
[176] http://www.invitrogen.com.
[177] http://www.atto-tec.com.
[178] S. Thomas, K. Ulrich, R. Daniel, N. Uli, *Single Mol.* **2002**, *3*, 327.
[179] K. Peneva, G. Mihov, A. Herrmann, N. Zarrabi, M. Borsch, M. Duncan Thomas, K. Müllen, *J. Am. Chem. Soc.* **2008**, *130*, 5398.
[180] K. Peneva, G. Mihov, F. Nolde, S. Rocha, J.-i. Hotta, K. Braeckmans, J. Hofkens, H. Uji-i, A. Herrmann, K. Müllen, *Angew. Chem.* **2008**, *120*, 3420; *Angew. Chem. Int. Ed.* **2008**, *47*, 3372.
[181] C. R. Goldsmith, J. Jaworski, M. Sheng, S. J. Lippard, *J. Am. Chem. Soc.* **2006**, *128*, 418.
[182] S. Lata, M. Gavutis, R. Tampe, J. Piehler, *J. Am. Chem. Soc.* **2006**, *128*, 2365.
[183] A. N. Kapanidis, Y. W. Ebright, R. H. Ebright, *J. Am. Chem. Soc.* **2001**, *123*, 12123.
[184] C. Joo, H. Balci, Y. Ishitsuka, C. Buranachai, T. Ha, *Annu. Rev. Biochem.* **2008**, *77*, 51.
[185] S. Rocha, A. Hutchison James, K. Peneva, A. Herrmann, K. Müllen, M. Skjot, I. Jorgensen Christian, A. Svendsen, F. C. De Schryver, J. Hofkens, H. Uji-i, *ChemPhysChem* **2009**, *10*, 151.
[186] R. Kasper, M. Heilemann, P. Tinnefeld, M. Sauer, "Towards ultra-stable fluorescent dyes for single-molecule spectroscopy," in *Biophotonics 2007: Optics in Life Science* (Eds.: J. Popp, G. von Bally), *Vol. 6633 of Proceedings of SPIE-OSA Biomedical Optics* (Optical Society of America, **2007**), Paper 6633_71.
[187] R. Prekeris, J. Klumperman, R. H. Scheller, Molecules *Molecular Cell* **2000**, *6*, 1437.

[188] M. Belting, *Trends Biochem. Sci.* **2003**, *28*, 145.
[189] K. Hizume, S. H. Yoshimura, K. Takeyasu, *Biochemistry* **2005**, *44*, 12978.
[190] M. Yin, R. Bauer, M. Klapper, K. Müllen, *Macromol. Chem. Phys.* **2007**, *208*, 1646.
[191] M. Yin, K. Ding, R. Gropeanu, J. Shen, R. Berger, T. Weil, K. Müllen, *Biomacromolecules* **2008**, *9*, 3231.
[192] M. Yin, C. Kuhlmann, K. Sorokina, C. Li, G. Mihov, E. Pietrowski, K. Koynov, M. Klapper, H. Luhmann, K. Müllen, T. Weil, *Biomacromolecules* **2008**, *9*, 1381.
[193] M. Yin, J. Shen, R. A. Gropeanu, G. O. Pflugfelder, T. Weil, K. Müllen, *Small* **2008**, *4*, 894.
[194] M. Yin, J. Shen, G. O. Pflugfelder, K. Müllen, *J. Am. Chem. Soc.* **2008**, *130*, 7806.